





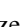
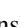



## Shower of $\gamma$ rays in the decay of the $49/2^+$ isomeric state in $^{147}\text{Gd}$

R. Broda <sup>1,\*</sup> J. Wrzesinski <sup>1</sup> C. Michelagnoli <sup>2,3,†</sup> S. Lunardi <sup>2,3</sup> C. Ur <sup>3,‡</sup> D. Bazzacco <sup>3</sup>  
R. Menegazzo <sup>3</sup> D. Mengoni <sup>2,3</sup> and F. Recchia <sup>2,3</sup>

<sup>1</sup>*Niewodniczański Institute of Nuclear Physics, Polish Academy of Science, Kraków PL-31-342, Poland*

<sup>2</sup>*Dipartimento di Fisica e Astronomia dell' Università degli Studi di Padova, Padova 35131, Italy*

<sup>3</sup>*Istituto Nazionale di Fisica Nucleare, Sezione di Padova, Padova 35131, Italy*



(Received 15 January 2020; revised manuscript received 16 March 2020; accepted 29 May 2020; published 24 June 2020)

Decay of the  $49/2^+$ ,  $0.51 \mu\text{s}$  isomeric state in  $^{147}\text{Gd}$  was reinvestigated in the  $\gamma$ -coincidence catcher experiment using the  $^{76}\text{Ge}(^{76}\text{Ge}, 5n)$  reaction and the GASP  $\gamma$  detector array. A previously suggested extraordinary complexity of the decay was confirmed and established down to intensity level better than  $10^{-3}$ /decay, involving 400 transitions and 89 levels populated between the isomer and the  $^{147}\text{Gd}$  ground state. The earlier measured electron conversion coefficients (ECC) and  $\gamma$  angular distributions, together with the total ECC extracted presently for low-energy transitions from the intensity balance, allowed to assign spin and parity values to all of the observed levels. Discussion of the level structure is restricted to few important cases clarified by the present investigation in the low-energy part of the decay scheme. Those involved the identification of the new  $M2$  and  $E2$  branches populating two new levels in the decay of the  $27/2^-$  isomer and firm location of positive parity levels arising in the coupling of this isomer with the  $3^-$  core excitation. In the upper part it was concluded that the observed complexity of the decay is initiated by fast low-energy  $M1$  transitions populating a group of similar structure levels located within 7.8–8.0 MeV excitation energy range. Some statistical features of the observed complex isomeric decay are reviewed and discussed.

DOI: [10.1103/PhysRevC.101.064320](https://doi.org/10.1103/PhysRevC.101.064320)

### I. INTRODUCTION

Identification of the  $3^-$  level as the lowest excited state in  $^{146}\text{Gd}$  [1] and subsequent placement of the first  $2^+$  level at nearly 400 keV higher energy [2] indicated subshell closure at the  $Z = 64$  proton number and qualified  $^{146}\text{Gd}$  as one of the doubly magic nuclei. This finding has initiated spectroscopic investigation in the region, which revealed simple shell-model structure of levels, as well as a frequent occurrence of isomeric states in all of the studied isotones with  $N = 81, 82$ , and  $83$  neutron numbers, e.g., Refs. [3–8]. In this series one of the best studied nuclei is the  $N = 83$   $^{147}\text{Gd}$  isotope, which is also the main object of the present work investigation. Initially, a sequence of medium spin yrast states in  $^{147}\text{Gd}$  was established as arising from the coupling of the  $f_{7/2}$  neutron with  $^{146}\text{Gd}$  core excitations, up to the maximum aligned  $\pi(h_{11/2})^2\nu f_{7/2}$  configuration of the  $27/2^-$  isomeric state ( $T_{1/2} = 27$  ns) [3]. Later, in the study of higher-lying levels, a long-lived ( $T_{1/2} = 510$  ns) high-spin isomer was identified. The history of this isomeric decay investigation will be summarized below as

the starting point of a much more detailed study performed in the present work. In the higher spin and excitation energy ranges above the isomer, the  $^{147}\text{Gd}$  level scheme has also been established and displayed irregularities typical for the shell-model structure [9,10] similar to the ones observed below the isomer. Finally, experiments aimed to search for the superdeformation phenomenon revealed six regular rotational bands and provided evidence that also these collective effects occur in  $^{147}\text{Gd}$  at very high spin values [11,12]. However, neither spin values, nor excitation energies of superdeformed states have been established, since transitions linking to the known normal deformation states could not be detected.

In the present work the  $49/2^+$  isomeric state in  $^{147}\text{Gd}$  was reinvestigated with the main goal to resolve an extraordinary and puzzling complexity of its decay that has been concluded but remained unresolved in the earlier study. The isomer was first observed in a broad experimental search for the existence of yrast traps [13]. In this search only a group of nuclei in the  $^{146}\text{Gd}$  region did show a presence of high-spin isomers and the prominent example was the previously unknown  $^{147}\text{Gd}$  isomer, which was estimated to decay with 100(50) ns half-life [13]. Later, in the spectroscopic study using  $(\alpha, 6n)$  reaction, the population of the same  $^{147}\text{Gd}$  high-spin isomer was reported [14], although the measured half-life of 560(60) ns was much longer. Due to the weak population only the most intense transitions could then be observed and a very tentative and incomplete decay scheme was proposed. Nevertheless, it was concluded that the isomer spin cannot be higher than

\* rafal.broda@ifj.edu.pl

† Present address: Institut Laue-Langevin, F-38042 Grenoble Cedex, France.

‡ Present address: IFINHH, P.O. BOX MG-6, Bucharest-Magurele, Romania.

$I = 49/2$ , and, in analogy to structures observed at lower energies, the shell-model interpretation was anticipated. Subsequently, the precise value of the measured  $g$  factor [15] defined the most probable structure of the isomer involving two protons and three neutrons with spins aligned to  $I = 49/2^+$  with  $[\pi d_{5/2}^{-2} h_{11/2}^2]10 [v h_{11/2}^{-1} i_{13/2} f_{7/2}]29/2$  configuration. The quadrupole moment has also been measured [16], its negative sign determined [17] and as expected for the state structure with five aligned particles, a  $\beta_2 = -0.19$  oblate deformation was concluded. A much more complete study of the isomeric decay was then performed in two independent experimental efforts. In the first one the  $^{147}\text{Gd}$  was investigated using ( $\alpha, 6n$ ) and ( $^{12}\text{C}, 5n$ ) reactions [18], which established the essential part of the level scheme and clarified the main decay paths of the isomer. A few months later results of a similar  $^{147}\text{Gd}$  study using ( $^{16}\text{O}, 4n$ ) and ( $^{28}\text{Si}, 5n$ ) reactions were published [19] and displayed satisfactory agreement of the level schemes concluded in both studies. The level scheme proposed in Ref. [18] was more complete, with 38 levels and only 12 unplaced transitions out of 86 identified in the isomeric decay. Also the transition ordering in some cascades was better controlled and accuracy of angular distribution results helped in spin-parity assignments. Whereas in Ref. [19] only 31 levels were located and 33 transitions out of 83 identified ones remained unplaced, the observed main decay paths established uniquely the excitation energy of the isomer and most of the levels populated in its decay. Apart from the independent  $\gamma$  angular distribution results, which were in general agreement with those of Ref. [18], the electron conversion coefficients measured in Ref. [19] provided the most valuable input for spin-parity assignments. In particular these results allowed us to assign firmly the isomer as  $I^\pi = 49/2^+$ , i.e., one unit higher than (47/2) tentatively suggested in Ref. [18].

In both studies a significant imbalance of the decay intensity was noted in the high-energy part of the isomeric decay. In Fig. 3 of Ref. [18] the quantitative analysis of this effect shows that in the 8–5 MeV excitation energy range only a fraction of the initial isomeric decay intensity is observed and a large part of it remains undetected. Whereas the intensity imbalance is gradually smaller at lower excitation energies down to 5 MeV, in the region of about 7.5 MeV the fraction of the missing intensity was larger than 60%. Taking into account the intensity detection threshold, it has been concluded that for several levels below 8 MeV an extraordinary  $\gamma$ -decay branching must occur. It was estimated that this branching may involve at least 50 different transition cascades, each of them carrying less than 1% intensity of the isomeric decay. The clarification of this puzzling feature was the main motivation of the present work study. It was anticipated that the presently available spectroscopy tools will enable to find the missing isomeric decay intensity, as well as to check and possibly correct inconsistencies of results reported in the two previous studies [18,19]. All of the results outlined above have been reviewed and summarized in the NDS [20]. The measured electron conversion coefficients, as well as  $\gamma$  angular distribution results served as important input in the final spin-parity assignments of levels established in the present study. The isomeric half-lives of 26.8(7) ns and 510(20) ns for

the  $27/2^-$  and  $49/2^+$  isomers, respectively, were also adopted from Ref. [20].

## II. EXPERIMENTAL PROCEDURE

The experiment was performed in the Legnaro National Laboratory (Italy) using the 290 MeV  $^{76}\text{Ge}$  beam from the Tandem-ALPI accelerators and the GASP  $\gamma$ -detector array in configuration II [21], i.e., without the inner BGO ball, thereby allowing the 40 Compton suppressed HP Ge detectors to be much closer (23 cm) to the center of the reaction chamber, which was surrounded by a spherical Pb shield acting as collimator. The  $^{147}\text{Gd}$  was produced in a symmetric fusion evaporation reaction  $^{76}\text{Ge}(^{76}\text{Ge}, 5n)$  with the 290 MeV beam energy selected as optimal for the  $49/2^+$  isomer population. The recoiling reaction products were collected in the 99.9% enriched  $^{208}\text{Pb}$  catcher placed in the center of the GASP array. The self-supporting 0.8 mg/cm<sup>2</sup>, 99% enriched  $^{76}\text{Ge}$  target, located 16 cm upstream, was shielded with a thick movable Pb cylinder placed in the beam tube to exclude detection of prompt  $\gamma$  rays emitted directly from the target. In the later analysis, testing the feasibility of such experimental setup to study secondary Coulomb excitation of reaction products recoiling into the catcher, it was found that only six detectors placed at the most forward angles could detect with their edges a very weak Doppler shifted prompt  $\gamma$  transitions from the target. Essentially, the collected coincidence data were free of such contribution and included events arising solely from isomeric decays occurring in the reaction products stopped in the catcher. The flight time of 11.5 ns estimated for the reaction products to reach the catcher did not affect much the yield of the  $^{147}\text{Gd}$  isomer, but reduced significantly the presence of isomers with shorter half-lives, which made the  $^{147}\text{Gd}$  data even cleaner. The data analysis allowed us to estimate quantitatively yields of the reaction products collected in the catcher. With 100 units assigned to the  $^{147}\text{Gd}$  isomer, the  $^{148}\text{Gd}$ , and  $^{146}\text{Gd}$  isomers arising in  $4n$  and  $6n$  evaporation channels were observed with yields 20 and 7, respectively. Also the high-spin  $49/2^+$  isomer in  $^{145}\text{Sm}$  [22] populated in the ( $\alpha, 3n$ ) evaporation channel could be observed with six units yield and a relatively large 12 units contribution was determined for the  $^{88}\text{Zr}$  produced by the  $^{76}\text{Ge}$  beam colliding with the  $^{16}\text{O}$  present in catcher surface layer. Apart from the  $^{145}\text{Sm}$  isomer, all other observed isomeric decays are very simple and could be easily controlled in the analysis of  $\gamma$  coincidence data with this predominance of  $^{147}\text{Gd}$  events. Also the statistics of the collected data was satisfactory and allowed us to resolve many details of the complex isomeric decay.

Double- and higher-fold  $\gamma$  coincidences were measured with an ordinary set of energy and time parameters. Cu absorbers placed in front of detectors and lowering of the CFD thresholds enabled observation of the low-energy transitions down to the Gd KX-ray energy. Special care was devoted to calibrate the detector efficiency and to check the summing effects, thereby controlling the crossover transition intensities. In the effective three-day run with beam on target,  $10^9$   $\gamma$  coincidence events were collected and sorted with the required conditions in subsequent off-beam analysis.

### III. ISOMERIC DECAY SCHEME

In a standard way the collected  $\gamma$ -coincidence events were sorted into  $\gamma\gamma$  matrices and  $\gamma\gamma\gamma$  cubes selecting various conditions on time parameters. Since no other level with nanosecond or longer half-life could be observed in the whole decay range between the  $49/2^+$  and the known lower-lying isomers, only the 27 ns half-life of the  $27/2^-$  isomer was exploited to select delayed coincidences, which distinguished transitions located below, above, and those passing by the isomer. Particularly clean and useful was the  $\gamma\gamma$  matrix involving transitions above this isomer, which were selected by requiring delayed coincidences with all intense transitions occurring in the  $27/2^-$  isomer decay. However, in the main  $\gamma$ -coincidence analysis essentially two sets of  $\gamma\gamma$  matrices and  $\gamma\gamma\gamma$  cubes were used with selection of the narrow (0–20 ns) or broad (0–70 ns) prompt time windows allowing us to reduce or fully involve transitions below the  $27/2^-$  isomer, respectively. Whereas the  $\gamma\gamma\gamma$  cube analysis established detailed coincidence relationships necessary to construct the decay scheme, the double coincidence  $\gamma\gamma$  matrices provided much higher statistics to determine safely relative intensities of many weaker transitions and to check later the intensity balance at each level.

With the detection threshold reaching often well below the transition intensity  $10^{-3}$  per decay, a very complete decay scheme was established involving 89 populated levels and 400  $\gamma$  transitions firmly placed between the  $49/2^+$  isomer and the  $7/2^-$  ground state. All of these  $\gamma$  transitions are listed in Table I in increasing energy order, with intensities normalized to 1000 units of the total isomer decay intensity and placement indicated by the initial level energy  $E_i$ .

Table II gives the list of transitions for which the total electron conversion coefficients could be extracted from the intensity balance observed in the appropriately selected coincidence spectra. These results together with the earlier reported angular distribution results [18,19] and the measured electron conversion coefficients [19] provided spin-parity assignments for most of the strongly populated levels and subsequently served to assign also weaker populated levels on the basis of the observed feeding and depopulation branches.

The complete decay scheme divided into two parts is displayed in Fig. 1 (top part), and Fig. 2 (bottom part) to demonstrate an extraordinary complexity rather than providing transparency of details. Essentially, all of the levels and transitions established in the present study of this decay are included in the figures and for strong transitions intensities are indicated by the arrow thickness. Whereas the detailed inspection of the decay flow might be limited, the figures provide general view of the observed  $\gamma$ -ray shower. In the lower-energy part (Fig. 2) the well-established simple sequence of yrast levels represents the bulk part of the decay intensity. Some new observations in this part will be discussed later as selected examples of the observed level structure. In the upper energy part (Fig. 1) one clearly observes the development of the increasing decay fragmentation, when the isomer decay intensity is shared between a large number of decay ways creating the  $\gamma$ -ray shower. The observed decay features and simple statistical considerations will be later briefly discussed.

TABLE I. List of  $\gamma$  transitions identified in the  $49/2^+$  isomer decay in  $^{147}\text{Gd}$ . Uncertainty of transition energies listed in the first column is 0.1 keV, unless indicated. Relative  $\gamma$ -transition intensities listed in the second column are normalized to 1000 units attributed to the total isomeric decay intensity including electron conversion. Intensities of transitions below the  $27/2^-$  isomer were reduced to exclude direct population of this isomer in reaction. Energies and spin-parity assignments of initial levels are given in the last two columns.

| $E_\gamma$ (keV) | $I_\gamma$ (keV)      | $E_i$ (keV) | $J^\pi$           |
|------------------|-----------------------|-------------|-------------------|
| 12.1             | 0.024(1) <sup>a</sup> | 6906.7      | 41/2 <sup>+</sup> |
| 30.4             | 6.5(8) <sup>a</sup>   | 7994.2      | 43/2 <sup>-</sup> |
| 48.3             | 6.4(9) <sup>a</sup>   | 7873.9      | 41/2 <sup>-</sup> |
| 57.4(3)          | 1.5(1)                | 5029.0      | 33/2 <sup>+</sup> |
| 68.0(2)          | 0.8(2)                | 6906.7      | 41/2 <sup>+</sup> |
| 71.8             | 1.0(2) <sup>a</sup>   | 3581.7      | 27/2 <sup>-</sup> |
| 72.7             | 14(3)                 | 7873.9      | 41/2 <sup>-</sup> |
| 73.7             | 1.8(6)                | 7873.9      | 41/2 <sup>-</sup> |
| 73.7(3)          | 0.3(1)                | 7669.6      | 39/2 <sup>-</sup> |
| 77.2(3)          | 0.4(1) <sup>a</sup>   | 7994.2      | 43/2 <sup>-</sup> |
| 80.4             | 43.3(46)              | 5029.0      | 33/2 <sup>+</sup> |
| 83.9             | 63.1(24)              | 2572.1      | 19/2 <sup>-</sup> |
| 90.8             | 0.9(2)                | 7994.2      | 43/2 <sup>-</sup> |
| 105.5(3)         | 0.4(2)                | 7873.9      | 41/2 <sup>-</sup> |
| 109.0(3)         | 1.1(3)                | 7801.3      | 41/2 <sup>-</sup> |
| 110.0            | 26.5(17)              | 3691.7      | 25/2 <sup>-</sup> |
| 117.2            | 178(7)                | 5382.1      | 33/2 <sup>-</sup> |
| 119.8(3)         | 0.8(4)                | 7825.6      | 41/2 <sup>-</sup> |
| 120.2            | 223(17)               | 7994.2      | 43/2 <sup>-</sup> |
| 140.6            | 1.7(2)                | 7035.2      | 41/2 <sup>+</sup> |
| 146.8(2)         | 2.8(3)                | 5264.9      | 31/2 <sup>-</sup> |
| 155.5            | 1.5(3)                | 7873.9      | 41/2 <sup>-</sup> |
| 155.5(3)         | 0.6(2)                | 6471.3      | 39/2 <sup>-</sup> |
| 157.5            | 14.5(7)               | 6621.2      | 39/2 <sup>+</sup> |
| 159.7            | 80.4(23)              | 4229.8      | 29/2 <sup>-</sup> |
| 162.4(3)         | 0.9(4)                | 7963.8      | 43/2 <sup>-</sup> |
| 168.2(3)         | 0.4(1)                | 7873.9      | 41/2 <sup>-</sup> |
| 168.6            | 26.7(11)              | 7994.2      | 43/2 <sup>-</sup> |
| 168.6(2)         | 1.3(3)                | 6181.3      | 35/2 <sup>+</sup> |
| 173.4            | 1.3(3)                | 6894.5      | 39/2 <sup>+</sup> |
| 177.0(3)         | 2.0(6)                | 7389.3      | 43/2 <sup>+</sup> |
| 179.8            | 1.4(3)                | 8333.3      | 45/2 <sup>+</sup> |
| 181.8(2)         | 12.1(33)              | 3691.7      | 25/2 <sup>-</sup> |
| 182.9            | 670(20)               | 3581.7      | 27/2 <sup>-</sup> |
| 185.2(3)         | 6.4(9)                | 5029.0      | 33/2 <sup>+</sup> |
| 188.1            | 155(8)                | 2760.2      | 21/2 <sup>+</sup> |
| 192.2(3)         | 1.0(3)                | 6373.2      | 37/2 <sup>-</sup> |
| 192.9            | 32.3(17)              | 7994.2      | 43/2 <sup>-</sup> |
| 193.9(5)         | 0.2(1)                | 7994.2      | 43/2 <sup>-</sup> |
| 196.6            | 5.1(3)                | 7035.2      | 41/2 <sup>+</sup> |
| 200.7            | 470(22)               | 5582.8      | 35/2 <sup>-</sup> |
| 204.4            | 9.1(9)                | 7873.9      | 41/2 <sup>-</sup> |
| 205.4(3)         | 3.0(4)                | 7801.3      | 41/2 <sup>-</sup> |
| 207.4            | 29.8(11)              | 8333.3      | 45/2 <sup>+</sup> |
| 207.7            | 8.3(6)                | 7873.9      | 41/2 <sup>-</sup> |
| 212.6(3)         | 1.3(4)                | 3398.8      | 25/2 <sup>+</sup> |
| 213.3(2)         | 1.2(2)                | 5652.6      | 33/2 <sup>-</sup> |
| 223.0            | 26.8(8)               | 4229.8      | 29/2 <sup>-</sup> |
| 228.1            | 7.3(6)                | 7873.9      | 41/2 <sup>-</sup> |

TABLE I. (*Continued.*)

| $E_\gamma$ (keV) | $I_\gamma$ (keV)     | $E_i$ (keV) | $J^\pi$           |
|------------------|----------------------|-------------|-------------------|
| 229.7            | 4.9(7)               | 7825.6      | 41/2 <sup>-</sup> |
| 236.1(2)         | 2.3(4)               | 5264.9      | 31/2 <sup>-</sup> |
| 236.2            | 8.2(2)               | 8333.3      | 45/2 <sup>+</sup> |
| 239.6            | 10.3(7)              | 6936.7      | 39/2 <sup>+</sup> |
| 245.8(5)         | 0.6(3)               | 6012.8      | 35/2 <sup>+</sup> |
| 247.3(2)         | 1.1(3)               | 7917.0      | 41/2 <sup>-</sup> |
| 248.1(2)         | 3.9(7)               | 6621.2      | 39/2 <sup>+</sup> |
| 248.4            | 5.0(6)               | 6906.7      | 41/2 <sup>+</sup> |
| 254.4            | 828(25) <sup>b</sup> | 8587.7      | 49/2 <sup>+</sup> |
| 264.0            | 2.3(3)               | 5382.1      | 33/2 <sup>-</sup> |
| 270.4            | 16.3(13)             | 6012.8      | 35/2 <sup>+</sup> |
| 272.1            | 767(33)              | 2760.2      | 21/2 <sup>+</sup> |
| 277.8            | 796(33)              | 3038.0      | 23/2 <sup>+</sup> |
| 278.0            | 1.7(9)               | 7873.9      | 41/2 <sup>-</sup> |
| 279.6(3)         | 0.6(2)               | 4617.8      | 29/2 <sup>+</sup> |
| 282.6            | 8.3(9)               | 6463.8      | 37/2 <sup>+</sup> |
| 283.5            | 1.1(2)               | 7669.6      | 39/2 <sup>-</sup> |
| 285.2(3)         | 5.3(7)               | 6658.4      | 39/2 <sup>-</sup> |
| 285.4            | 114(4)               | 6906.7      | 41/2 <sup>+</sup> |
| 288.3            | 1.7(6)               | 7994.2      | 43/2 <sup>-</sup> |
| 291.9(3)         | 1.0(3)               | 6373.2      | 37/2 <sup>-</sup> |
| 293.0(3)         | 1.0(3)               | 5264.9      | 31/2 <sup>-</sup> |
| 293.0(2)         | 5.0(6)               | 3691.7      | 25/2 <sup>-</sup> |
| 297.8            | 2.3(3)               | 7963.8      | 43/2 <sup>-</sup> |
| 299.1            | 6.7(4)               | 6621.2      | 39/2 <sup>+</sup> |
| 302.4(3)         | 0.6(3)               | 7994.2      | 43/2 <sup>-</sup> |
| 303.1(2)         | 2.8(4)               | 6315.7      | 37/2 <sup>+</sup> |
| 303.5(2)         | 2.8(3)               | 4533.5      | 29/2 <sup>-</sup> |
| 306.9            | 2.0(6)               | 5959.6      | 35/2 <sup>-</sup> |
| 310.2(3)         | 1.1(3)               | 4843.7      | 31/2 <sup>-</sup> |
| 312.0(4)         | 0.4(2)               | 7619.7      | 41/2 <sup>+</sup> |
| 315.0            | 24.4(9)              | 4006.6      | 27/2 <sup>-</sup> |
| 316.0(2)         | 4.9(9)               | 5264.9      | 31/2 <sup>-</sup> |
| 317.8            | 3.5(4)               | 7212.6      | 41/2 <sup>-</sup> |
| 317.9            | 9.4(4)               | 5582.8      | 35/2 <sup>-</sup> |
| 322.1            | 5.0(6)               | 4533.5      | 29/2 <sup>-</sup> |
| 323.8            | 1.4(3)               | 3510.0      | 23/2 <sup>-</sup> |
| 326.8            | 6.0(6)               | 6894.5      | 39/2 <sup>+</sup> |
| 327.9            | 6.3(8)               | 7994.2      | 43/2 <sup>-</sup> |
| 330.8            | 245(7)               | 4948.6      | 31/2 <sup>+</sup> |
| 339.2            | 783(24)              | 8333.3      | 45/2 <sup>+</sup> |
| 340.1            | 513(33)              | 5922.9      | 37/2 <sup>-</sup> |
| 344.0(3)         | 2.2(3)               | 7963.8      | 43/2 <sup>-</sup> |
| 350.0            | 3.5(3)               | 5622.1      | 33/2 <sup>+</sup> |
| 352.9            | 26.3(13)             | 5382.1      | 33/2 <sup>-</sup> |
| 354.0(3)         | 0.4(2)               | 8125.9      | 43/2 <sup>+</sup> |
| 354.0            | 7.9(6)               | 7389.3      | 43/2 <sup>+</sup> |
| 360.2            | 13.5(10)             | 6012.8      | 35/2 <sup>+</sup> |
| 360.8            | 685(28)              | 3398.8      | 25/2 <sup>+</sup> |
| 369.0            | 30.2(18)             | 6936.7      | 39/2 <sup>+</sup> |
| 369.4            | 59.8(25)             | 8333.3      | 45/2 <sup>+</sup> |
| 374.2            | 10.5(7)              | 7212.6      | 41/2 <sup>-</sup> |
| 374.5            | 3.0(6)               | 7994.2      | 43/2 <sup>-</sup> |
| 374.8            | 6.0(13)              | 6838.4      | 39/2 <sup>+</sup> |
| 375.0(2)         | 0.9(2)               | 6697.1      | 37/2 <sup>+</sup> |
| 378.4            | 115(3)               | 4070.1      | 27/2 <sup>-</sup> |

TABLE I. (*Continued.*)

| $E_\gamma$ (keV) | $I_\gamma$ (keV)      | $E_i$ (keV) | $J^\pi$           |
|------------------|-----------------------|-------------|-------------------|
| 380.7(2)         | 2.6(4)                | 4450.6      | 29/2 <sup>-</sup> |
| 381.5            | 5.5(6)                | 8153.4      | 45/2 <sup>+</sup> |
| 382.8(3)         | 0.9(3)                | 6463.8      | 37/2 <sup>+</sup> |
| 384.5(3)         | 0.6(2)                | 7691.9      | 41/2 <sup>+</sup> |
| 385.4(2)         | 4.4(10)               | 5767.3      | 35/2 <sup>-</sup> |
| 390.5            | 7.8(3)                | 6012.8      | 35/2 <sup>+</sup> |
| 393.1            | 30.6(20)              | 4843.7      | 31/2 <sup>-</sup> |
| 395.5            | 12.6(9)               | 3581.7      | 27/2 <sup>-</sup> |
| 403.5(1)         | 4.3(4)                | 7126.6      | 39/2 <sup>-</sup> |
| 406.5            | 6.0(6)                | 4617.8      | 29/2 <sup>+</sup> |
| 410.4(3)         | 0.9(3)                | 6181.3      | 35/2 <sup>+</sup> |
| 410.4            | 23.8(10)              | 5382.1      | 33/2 <sup>-</sup> |
| 413.7(2)         | 2.8(7)                | 6373.2      | 37/2 <sup>-</sup> |
| 414.0            | 146(6)                | 7035.2      | 41/2 <sup>+</sup> |
| 415.2            | 9.1(6)                | 4948.6      | 31/2 <sup>+</sup> |
| 419.7(3)         | 1.2(3)                | 7771.9      | 43/2 <sup>+</sup> |
| 421.2            | 74.0(22)              | 5264.9      | 31/2 <sup>-</sup> |
| 423.2            | 5.2(7)                | 6894.5      | 39/2 <sup>+</sup> |
| 424.9            | 104(3)                | 4006.6      | 27/2 <sup>-</sup> |
| 425.9            | 33.1(3)               | 3186.1      | 23/2 <sup>+</sup> |
| 428.7(3)         | 1.5(3)                | 6081.4      | 35/2 <sup>-</sup> |
| 430.0(3)         | 0.4(2)                | 6012.8      | 35/2 <sup>+</sup> |
| 430.8            | 2.4(4)                | 6894.5      | 39/2 <sup>+</sup> |
| 433.1            | 11.3(9)               | 7963.8      | 43/2 <sup>-</sup> |
| 433.6            | 8.3(9)                | 5382.1      | 33/2 <sup>-</sup> |
| 434.5            | 57.8(42) <sup>b</sup> | 8587.7      | 49/2 <sup>+</sup> |
| 435.3            | 126(6)                | 6906.7      | 41/2 <sup>+</sup> |
| 440.1            | 2.4(3)                | 6621.2      | 39/2 <sup>+</sup> |
| 444.0            | 51.9(17)              | 4450.6      | 29/2 <sup>-</sup> |
| 459.5            | 2.2(6)                | 7396.0      | 41/2 <sup>+</sup> |
| 463.3            | 15.8(9)               | 7994.2      | 43/2 <sup>-</sup> |
| 463.4            | 28.7(15)              | 4533.5      | 29/2 <sup>-</sup> |
| 465.4            | 5.4(6)                | 6936.7      | 39/2 <sup>+</sup> |
| 470.0            | 4.2(3)                | 5742.2      | 33/2 <sup>+</sup> |
| 471.9(2)         | 3.8(3)                | 3510.0      | 23/2 <sup>-</sup> |
| 472.7(3)         | 0.3(2)                | 6936.7      | 39/2 <sup>+</sup> |
| 482.6            | 99.5(23)              | 7389.3      | 43/2 <sup>+</sup> |
| 488.0            | 1.9(3)                | 7873.9      | 41/2 <sup>-</sup> |
| 488.4            | 5.1(4)                | 4070.1      | 27/2 <sup>-</sup> |
| 498.0            | 23.8(17)              | 4948.6      | 31/2 <sup>+</sup> |
| 501.5            | 4.9(6)                | 7396.0      | 41/2 <sup>+</sup> |
| 504.6            | 2.0(6)                | 6463.8      | 37/2 <sup>+</sup> |
| 505.5            | 21.2(12)              | 3691.7      | 25/2 <sup>-</sup> |
| 512.7(3)         | 1.8(3)                | 7530.8      | 41/2 <sup>+</sup> |
| 514.0            | 6.2(7)                | 7352.4      | 41/2 <sup>+</sup> |
| 517.8            | 3.2(4)                | 7825.6      | 41/2 <sup>-</sup> |
| 518.1(2)         | 2.9(4)                | 6833.7      | 37/2 <sup>-</sup> |
| 519.5(2)         | 4.2(7)                | 4211.4      | 27/2 <sup>-</sup> |
| 520.4            | 3.6(4)                | 5959.6      | 35/2 <sup>-</sup> |
| 520.9(2)         | 4.1(6)                | 4971.7      | 31/2 <sup>-</sup> |
| 526.1(3)         | 2.5(7)                | 7801.3      | 41/2 <sup>-</sup> |
| 526.8            | 9.2(6)                | 4533.5      | 29/2 <sup>-</sup> |
| 538.4            | 42.0(17)              | 5382.1      | 33/2 <sup>-</sup> |
| 539.4(3)         | 2.6(9)                | 7666.2      | 41/2 <sup>-</sup> |
| 540.9            | 27.9(10)              | 5922.9      | 37/2 <sup>-</sup> |
| 543.7            | 118(6)                | 3581.7      | 27/2 <sup>-</sup> |

TABLE I. (Continued.)

| $E_\gamma$ (keV) | $I_\gamma$ (keV)      | $E_i$ (keV) | $J^\pi$           |
|------------------|-----------------------|-------------|-------------------|
| 548.4            | 157(7)                | 6471.3      | 39/2 <sup>-</sup> |
| 548.5(2)         | 6.2(9)                | 6315.7      | 37/2 <sup>+</sup> |
| 550.3            | 2.4(6)                | 7825.6      | 41/2 <sup>-</sup> |
| 553.9            | 4.1(3)                | 5582.8      | 35/2 <sup>-</sup> |
| 554.8(3)         | 0.8(3)                | 6567.7      | 37/2 <sup>+</sup> |
| 557.6            | 3.1(3)                | 7396.0      | 41/2 <sup>+</sup> |
| 559.1(3)         | 1.7(3)                | 6181.3      | 35/2 <sup>+</sup> |
| 560.9            | 1.2(3)                | 7596.0      | 39/2 <sup>-</sup> |
| 561.6            | 2.4(3)                | 8333.3      | 45/2 <sup>+</sup> |
| 566.3            | 4.1(3)                | 7873.9      | 41/2 <sup>-</sup> |
| 567.9            | 5.6(4)                | 7963.8      | 43/2 <sup>-</sup> |
| 571.5            | 10.6(10)              | 7035.2      | 41/2 <sup>+</sup> |
| 574.5            | 10.7(6)               | 7963.8      | 43/2 <sup>-</sup> |
| 576.9(3)         | 1.8(4)                | 6658.4      | 39/2 <sup>-</sup> |
| 578.7            | 2.0(3)                | 6894.5      | 39/2 <sup>+</sup> |
| 584.5(2)         | 2.1(4)                | 7619.7      | 41/2 <sup>+</sup> |
| 591.1            | 33.0(13)              | 6906.7      | 41/2 <sup>+</sup> |
| 593.0(3)         | 1.0(3)                | 5622.1      | 33/2 <sup>+</sup> |
| 593.7            | 27.4(11) <sup>b</sup> | 8587.7      | 49/2 <sup>+</sup> |
| 598.2            | 19.1(10)              | 7994.2      | 43/2 <sup>-</sup> |
| 598.7            | 2.6(6)                | 7873.9      | 41/2 <sup>-</sup> |
| 605.0            | 28.8(15)              | 7994.2      | 43/2 <sup>-</sup> |
| 605.8(3)         | 4.0(8)                | 6373.2      | 37/2 <sup>-</sup> |
| 608.5            | 138(8)                | 6621.2      | 39/2 <sup>+</sup> |
| 611.2            | 18.3(8)               | 4617.8      | 29/2 <sup>+</sup> |
| 611.4            | 56.4(28)              | 5582.8      | 35/2 <sup>-</sup> |
| 614.0            | 49.7(20)              | 4843.7      | 31/2 <sup>-</sup> |
| 618.7            | 2.2(3)                | 7801.3      | 41/2 <sup>-</sup> |
| 620.9            | 1.5(2)                | 6936.7      | 39/2 <sup>+</sup> |
| 623.4(3)         | 0.8(3)                | 5652.6      | 33/2 <sup>-</sup> |
| 623.8(3)         | 1.3(3) <sup>b</sup>   | 8587.7      | 49/2 <sup>+</sup> |
| 630.7(2)         | 1.8(4)                | 6012.8      | 35/2 <sup>+</sup> |
| 636.3            | 8.1(9)                | 7530.8      | 41/2 <sup>+</sup> |
| 638.6            | 54.4(21)              | 3398.8      | 25/2 <sup>+</sup> |
| 641.8            | 2.6(4)                | 7994.2      | 43/2 <sup>-</sup> |
| 642.5            | 1.3(3)                | 6081.4      | 35/2 <sup>-</sup> |
| 645.0            | 4.6(6)                | 6567.7      | 37/2 <sup>+</sup> |
| 646.2(2)         | 3.0(3)                | 4338.0      | 27/2 <sup>-</sup> |
| 647.2(2)         | 6.1(8)                | 5264.9      | 31/2 <sup>-</sup> |
| 647.9(2)         | 4.6(6)                | 4229.8      | 29/2 <sup>-</sup> |
| 650.4(4)         | 0.4(2)                | 5622.1      | 33/2 <sup>+</sup> |
| 653.8            | 49.7(22)              | 3691.7      | 25/2 <sup>-</sup> |
| 654.4            | 6.0(4)                | 5272.1      | 31/2 <sup>-</sup> |
| 656.3            | 2.4(3)                | 7963.8      | 43/2 <sup>-</sup> |
| 660.4            | 1.8(4)                | 7124.2      | 39/2 <sup>-</sup> |
| 671.4            | 24.4(10)              | 4070.1      | 27/2 <sup>-</sup> |
| 673.6            | 3.1(4)                | 5622.1      | 33/2 <sup>+</sup> |
| 674.8(4)         | 0.8(4)                | 7801.3      | 41/2 <sup>-</sup> |
| 675.0(3)         | 0.7(3)                | 7396.0      | 41/2 <sup>+</sup> |
| 680.8            | 3.3(4)                | 5652.6      | 33/2 <sup>-</sup> |
| 686.7            | 5.5(4)                | 7994.2      | 43/2 <sup>-</sup> |
| 691.1            | 4.2(3)                | 7873.9      | 41/2 <sup>-</sup> |
| 692.3            | 8.4(9)                | 7530.8      | 41/2 <sup>+</sup> |
| 696.5            | 5.0(3)                | 6463.8      | 37/2 <sup>+</sup> |
| 698.3            | 187(8)                | 6621.2      | 39/2 <sup>+</sup> |
| 698.8            | 2.9(4)                | 7396.0      | 41/2 <sup>+</sup> |
| 698.9            | 3.3(1)                | 6658.4      | 39/2 <sup>-</sup> |

TABLE I. (Continued.)

| $E_\gamma$ (keV) | $I_\gamma$ (keV) | $E_i$ (keV) | $J^\pi$           |
|------------------|------------------|-------------|-------------------|
| 699.0(3)         | 1.2(4)           | 7825.6      | 41/2 <sup>-</sup> |
| 699.0(4)         | 1.1(6)           | 6081.4      | 35/2 <sup>-</sup> |
| 700.0(2)         | 1.7(3)           | 6322.0      | 35/2 <sup>+</sup> |
| 701.1(3)         | 0.8(2)           | 7825.6      | 41/2 <sup>-</sup> |
| 702.0(7)         | 0.8(3)           | 7596.0      | 39/2 <sup>-</sup> |
| 703.9            | 3.4(6)           | 6471.3      | 39/2 <sup>-</sup> |
| 704.0(3)         | 2.0(3)           | 5652.6      | 33/2 <sup>-</sup> |
| 713.4            | 1.7(3)           | 5742.2      | 33/2 <sup>+</sup> |
| 719.4            | 4.0(4)           | 7035.2      | 41/2 <sup>+</sup> |
| 721.3(5)         | 0.4(2)           | 7903.5      | 41/2 <sup>-</sup> |
| 733.2(3)         | 2.8(4)           | 6315.7      | 37/2 <sup>+</sup> |
| 736.6            | 8.1(7)           | 7771.9      | 43/2 <sup>+</sup> |
| 738.0            | 1.4(3)           | 7396.0      | 41/2 <sup>+</sup> |
| 738.2(3)         | 11.0(8)          | 5767.3      | 35/2 <sup>-</sup> |
| 739.8(4)         | 0.9(3)           | 7307.5      | 39/2 <sup>-</sup> |
| 741.3            | 14.5(8)          | 7212.6      | 41/2 <sup>-</sup> |
| 742.0(2)         | 6.5(3)           | 4971.7      | 31/2 <sup>-</sup> |
| 747.2(1)         | 17.3(6)          | 7873.9      | 41/2 <sup>-</sup> |
| 749.7(5)         | 0.7(2)           | 7873.9      | 41/2 <sup>-</sup> |
| 749.7(3)         | 5.5(8)           | 3510.0      | 23/2 <sup>-</sup> |
| 751.3            | 5.5(9)           | 7963.8      | 43/2 <sup>-</sup> |
| 756.2(2)         | 1.7(3)           | 4338.0      | 27/2 <sup>-</sup> |
| 759.1(2)         | 4.9(4)           | 4450.6      | 29/2 <sup>-</sup> |
| 762.7            | 1.7(4)           | 7596.0      | 39/2 <sup>-</sup> |
| 764.1            | 56.1(17)         | 8153.4      | 45/2 <sup>+</sup> |
| 765.9            | 2.8(3)           | 7801.3      | 41/2 <sup>-</sup> |
| 768.3(3)         | 0.9(3)           | 7389.3      | 43/2 <sup>+</sup> |
| 770.7(3)         | 1.1(6)           | 5742.2      | 33/2 <sup>+</sup> |
| 773.6            | 4.2(7)           | 8125.9      | 43/2 <sup>+</sup> |
| 778.4(2)         | 2.4(3)           | 5622.1      | 33/2 <sup>+</sup> |
| 781.3(2)         | 3.3(6)           | 7619.7      | 41/2 <sup>+</sup> |
| 781.7            | 15.8(8)          | 7994.2      | 43/2 <sup>-</sup> |
| 790.3            | 21.9(7)          | 7825.6      | 41/2 <sup>-</sup> |
| 790.3(2)         | 8.8(9)           | 6373.2      | 37/2 <sup>-</sup> |
| 793.8(3)         | 1.1(6)           | 5742.2      | 33/2 <sup>+</sup> |
| 795.7            | 10.5(8)          | 5767.3      | 35/2 <sup>-</sup> |
| 797.5(2)         | 1.1(3)           | 7691.9      | 41/2 <sup>+</sup> |
| 798.0(3)         | 1.7(6)           | 6721.0      | 37/2 <sup>-</sup> |
| 799.3(2)         | 2.3(3)           | 5771.0      | 33/2 <sup>-</sup> |
| 800.1            | 1.1(3)           | 6723.0      | 39/2 <sup>-</sup> |
| 800.5            | 2.3(6)           | 6567.7      | 37/2 <sup>+</sup> |
| 808.8(2)         | 1.4(3)           | 5652.6      | 33/2 <sup>-</sup> |
| 809.6(2)         | 2.2(3)           | 7182.7      | 39/2 <sup>+</sup> |
| 812.6(2)         | 14.0(8)          | 4211.4      | 27/2 <sup>-</sup> |
| 814.2            | 79.0(17)         | 5264.9      | 31/2 <sup>-</sup> |
| 820.8            | 8.3(6)           | 6833.7      | 37/2 <sup>-</sup> |
| 821.3            | 41.0(2)          | 3581.7      | 27/2 <sup>-</sup> |
| 821.4            | 4.9(9)           | 5272.1      | 31/2 <sup>-</sup> |
| 836.7(3)         | 5.6(6)           | 4843.7      | 31/2 <sup>-</sup> |
| 837.0(4)         | 0.6(3)           | 7963.8      | 43/2 <sup>-</sup> |
| 838.7            | 48.4(14)         | 7873.9      | 41/2 <sup>-</sup> |
| 843.5(4)         | 1.3(3)           | 7307.5      | 39/2 <sup>-</sup> |
| 848.7            | 43.9(17)         | 5382.1      | 33/2 <sup>-</sup> |
| 853.9(3)         | 1.0(4)           | 6621.2      | 39/2 <sup>+</sup> |
| 855.8(2)         | 2.0(3)           | 7873.9      | 41/2 <sup>-</sup> |
| 860.7(4)         | 0.8(4)           | 7182.7      | 39/2 <sup>+</sup> |
| 864.6            | 19.0(8)          | 7801.3      | 41/2 <sup>-</sup> |

TABLE I. (*Continued.*)

| $E_\gamma$ (keV) | $I_\gamma$ (keV)  | $E_i$ (keV) | $J^\pi$           |
|------------------|-------------------|-------------|-------------------|
| 865.2(3)         | 1.2(3)            | 7771.9      | 43/2 <sup>+</sup> |
| 867.0            | 7.2(6)            | 7182.7      | 39/2 <sup>+</sup> |
| 867.4(3)         | 2.0(6)            | 7994.2      | 43/2 <sup>-</sup> |
| 868.9            | 86.4(28)          | 4450.6      | 29/2 <sup>-</sup> |
| 880.8            | 4.2(7)            | 6463.8      | 37/2 <sup>+</sup> |
| 884.7(3)         | 0.9(3)            | 8097.1      | 43/2 <sup>+</sup> |
| 888.5            | 5.6(3)            | 6471.3      | 39/2 <sup>-</sup> |
| 888.7(3)         | 2.8(7)            | 7825.6      | 41/2 <sup>-</sup> |
| 894.6            | 14.0(13)          | 7801.3      | 41/2 <sup>-</sup> |
| 898.3            | 3.3(6)            | 5742.2      | 33/2 <sup>+</sup> |
| 906.0(3)         | 0.9(6)            | 5439.3      | 31/2 <sup>-</sup> |
| 906.7            | 21.5(10)          | 7801.3      | 41/2 <sup>-</sup> |
| 909.6            | 8.6(4)            | 7530.8      | 41/2 <sup>+</sup> |
| 913.3            | 2.2(2)            | 8125.9      | 43/2 <sup>+</sup> |
| 915.5            | 40.6(13)          | 6838.4      | 39/2 <sup>+</sup> |
| 919.0(3)         | 1.9(4)            | 7825.6      | 41/2 <sup>-</sup> |
| 923.8(3)         | 1.7(10)           | 5767.3      | 35/2 <sup>-</sup> |
| 924.1            | 7.1(6)            | 6936.7      | 39/2 <sup>+</sup> |
| 924.7            | 9.2(6)            | 7396.0      | 41/2 <sup>+</sup> |
| 927.2(2)         | 8.6(6)            | 5264.9      | 31/2 <sup>-</sup> |
| 928.6            | 23.0(17)          | 7963.8      | 43/2 <sup>-</sup> |
| 929.8            | 6.2(6)            | 6697.1      | 37/2 <sup>+</sup> |
| 937.2            | 40.0(19)          | 7873.9      | 41/2 <sup>-</sup> |
| 937.9(2)         | 18.2(10)          | 3510.0      | 23/2 <sup>-</sup> |
| 939.3(3)         | 3.9(6)            | 4338.0      | 27/2 <sup>-</sup> |
| 944.0            | 11.3(4)           | 8333.3      | 45/2 <sup>+</sup> |
| 951.7            | 11.2(7)           | 4533.5      | 29/2 <sup>-</sup> |
| 958.9            | 40.0(20)          | 7994.2      | 43/2 <sup>-</sup> |
| 962.9            | 3.1(6)            | 7801.3      | 41/2 <sup>-</sup> |
| 964.9(2)         | 4.0(7)            | 4971.7      | 31/2 <sup>-</sup> |
| 967.1            | 26.4(17)          | 7873.9      | 41/2 <sup>-</sup> |
| 967.6(3)         | 5.5(11)           | 7801.3      | 41/2 <sup>-</sup> |
| 971.6            | 46.4(17)          | 6894.5      | 39/2 <sup>+</sup> |
| 979.2            | 19.7(13)          | 7873.9      | 41/2 <sup>-</sup> |
| 983.8            | 51.6(18)          | 6012.8      | 35/2 <sup>+</sup> |
| 984.8            | 25.4(17)          | 6567.7      | 37/2 <sup>+</sup> |
| 987.3(3)         | 1.0(3)            | 7825.6      | 41/2 <sup>-</sup> |
| 991.8            | 14.8(9)           | 7307.5      | 39/2 <sup>-</sup> |
| 997.1            | 1000 <sup>b</sup> | 997.1       | 13/2 <sup>+</sup> |
| 998.5(2)         | 1.4(4)            | 7619.7      | 41/2 <sup>+</sup> |
| 1007.8(3)        | 0.9(3)            | 7666.2      | 41/2 <sup>-</sup> |
| 1011.4(3)        | 0.9(3)            | 7669.6      | 39/2 <sup>-</sup> |
| 1013.8(3)        | 2.0(4)            | 6936.7      | 39/2 <sup>+</sup> |
| 1035.4           | 7.2(7)            | 7873.9      | 41/2 <sup>-</sup> |
| 1036.1           | 245(7)            | 4617.8      | 29/2 <sup>+</sup> |
| 1038.3           | 3.3(17)           | 6621.2      | 39/2 <sup>+</sup> |
| 1040.4           | 5.5(9)            | 7873.9      | 41/2 <sup>-</sup> |
| 1047.5(2)        | 2.2(6)            | 7705.9      | 39/2 <sup>-</sup> |
| 1053.6(2)        | 7.3(8)            | 5264.9      | 31/2 <sup>-</sup> |
| 1057.1           | 87.4(23)          | 7963.8      | 43/2 <sup>-</sup> |
| 1061.9           | 6.5(3)            | 8097.1      | 43/2 <sup>+</sup> |
| 1064.3           | 56.5(23)          | 6012.8      | 35/2 <sup>+</sup> |
| 1065.0(3)        | 1.1(3)            | 7903.5      | 41/2 <sup>-</sup> |
| 1070.6(2)        | 2.0(3)            | 7691.9      | 41/2 <sup>+</sup> |
| 1079.1(2)        | 1.4(6)            | 7800.3      | 39/2 <sup>-</sup> |
| 1080.5(3)        | 1.0(3)            | 7396.0      | 41/2 <sup>+</sup> |
| 1087.4           | 36.2(11)          | 7994.2      | 43/2 <sup>-</sup> |

TABLE I. (*Continued.*)

| $E_\gamma$ (keV) | $I_\gamma$ (keV) | $E_i$ (keV) | $J^\pi$           |
|------------------|------------------|-------------|-------------------|
| 1090.7           | 15.9(4)          | 8125.9      | 43/2 <sup>+</sup> |
| 1095.1(2)        | 3.2(3)           | 7018.0      | 39/2 <sup>-</sup> |
| 1102.4(5)        | 0.7(3)           | 7825.6      | 41/2 <sup>-</sup> |
| 1104.3(4)        | 5.5(11)          | 7801.3      | 41/2 <sup>-</sup> |
| 1109.7(2)        | 1.3(2)           | 6081.4      | 35/2 <sup>-</sup> |
| 1114.3           | 8.4(4)           | 6697.1      | 37/2 <sup>+</sup> |
| 1118.1           | 4.7(4)           | 8153.4      | 45/2 <sup>+</sup> |
| 1124.4           | 11.4(8)          | 5742.2      | 33/2 <sup>+</sup> |
| 1132.1           | 2.4(6)           | 7596.0      | 39/2 <sup>-</sup> |
| 1138.2           | 4.1(3)           | 6721.0      | 37/2 <sup>-</sup> |
| 1140.2           | 4.0(3)           | 6723.0      | 39/2 <sup>-</sup> |
| 1152.1           | 3.0(6)           | 6181.3      | 35/2 <sup>+</sup> |
| 1152.2           | 98.5(31)         | 5382.1      | 33/2 <sup>-</sup> |
| 1155.8           | 3.0(6)           | 7619.7      | 41/2 <sup>+</sup> |
| 1167.9           | 2.9(3)           | 7825.6      | 41/2 <sup>-</sup> |
| 1180.2           | 42.0(17)         | 7801.3      | 41/2 <sup>-</sup> |
| 1190.2           | 2.1(2)           | 8097.1      | 43/2 <sup>+</sup> |
| 1194.9           | 14.2(8)          | 7666.2      | 41/2 <sup>-</sup> |
| 1195.0           | 10.8(10)         | 5264.9      | 31/2 <sup>-</sup> |
| 1198.0(3)        | 1.3(3)           | 7669.6      | 39/2 <sup>-</sup> |
| 1203.7(1)        | 16.7(10)         | 7126.6      | 39/2 <sup>-</sup> |
| 1204.5           | 7.5(9)           | 7825.6      | 41/2 <sup>-</sup> |
| 1215.7(3)        | 1.1(4)           | 7873.9      | 41/2 <sup>-</sup> |
| 1219.1(3)        | 1.9(6)           | 4617.8      | 29/2 <sup>+</sup> |
| 1219.2           | 13.1(4)          | 8125.9      | 43/2 <sup>+</sup> |
| 1232.7           | 7.6(7)           | 6181.3      | 35/2 <sup>+</sup> |
| 1237.6(2)        | 5.3(6)           | 6081.4      | 35/2 <sup>-</sup> |
| 1250.5(4)        | 2.3(10)          | 6833.7      | 37/2 <sup>-</sup> |
| 1252.7           | 37.4(13)         | 7873.9      | 41/2 <sup>-</sup> |
| 1258.2(2)        | 8.2(7)           | 5264.9      | 31/2 <sup>-</sup> |
| 1261.9           | 42.1(11)         | 4843.7      | 31/2 <sup>-</sup> |
| 1286.7(1)        | 54.9(19)         | 6315.7      | 37/2 <sup>+</sup> |
| 1293.0           | 4.3(6)           | 6322.0      | 35/2 <sup>+</sup> |
| 1298.1           | 3.6(4)           | 8333.3      | 45/2 <sup>+</sup> |
| 1329.0(3)        | 1.1(3)           | 7800.3      | 39/2 <sup>-</sup> |
| 1352.6           | 5.9(6)           | 7275.5      | 41/2 <sup>-</sup> |
| 1354.0           | 1.5(3)           | 7825.6      | 41/2 <sup>-</sup> |
| 1373.5           | 1.5(2)           | 6322.0      | 35/2 <sup>+</sup> |
| 1390.0           | 96.7(31)         | 4971.7      | 31/2 <sup>-</sup> |
| 1402.7(3)        | 0.9(1)           | 7718.4      | 39/2 <sup>-</sup> |
| 1422.8           | 10.8(6)          | 5652.6      | 33/2 <sup>-</sup> |
| 1426.1(3)        | 2.8(6)           | 5117.9      | 29/2 <sup>-</sup> |
| 1426.6           | 2.3(2)           | 8333.3      | 45/2 <sup>+</sup> |
| 1434.7           | 29.0(10)         | 6463.8      | 37/2 <sup>+</sup> |
| 1491.0           | 905(33)          | 2488.1      | 17/2 <sup>+</sup> |
| 1536.2(2)        | 5.9(6)           | 5117.9      | 29/2 <sup>-</sup> |
| 1538.8           | 3.0(4)           | 6567.7      | 37/2 <sup>+</sup> |
| 1575.1           | 93(3)            | 2572.1      | 19/2 <sup>-</sup> |
| 1668.2           | 1.5(3)           | 6697.1      | 37/2 <sup>+</sup> |
| 1683.3           | 218(8)           | 5264.9      | 31/2 <sup>-</sup> |
| 1709.8(3)        | 0.8(3)           | 7669.6      | 39/2 <sup>-</sup> |
| 1723.0(3)        | 0.8(2)           | 7645.8      | 39/2 <sup>-</sup> |
| 1795.2(5)        | 0.7(2)           | 7718.4      | 39/2 <sup>-</sup> |
| 1803.2           | 3.0(3)           | 7386.0      | 37/2 <sup>-</sup> |
| 1857.6           | 5.6(6)           | 5439.3      | 31/2 <sup>-</sup> |
| 1877.5           | 7.0(4)           | 7800.3      | 39/2 <sup>-</sup> |
| 1902.7           | 8.9(4)           | 7825.6      | 41/2 <sup>-</sup> |

TABLE I. (Continued.)

| $E_\gamma$ (keV) | $I_\gamma$ (keV) | $E_i$ (keV) | $J^\pi$           |
|------------------|------------------|-------------|-------------------|
| 1951.1           | 67.9(24)         | 7873.9      | 41/2 <sup>-</sup> |
| 1980.6           | 4.1(3)           | 7903.5      | 41/2 <sup>-</sup> |
| 1994.1           | 2.1(3)           | 7917.0      | 41/2 <sup>-</sup> |
| 2004.2(5)        | 0.6(2)           | 7386.0      | 37/2 <sup>-</sup> |
| 2013.0           | 4.2(3)           | 7596.0      | 39/2 <sup>-</sup> |
| 2063.0           | 5.9(3)           | 7645.8      | 39/2 <sup>-</sup> |
| 2086.8           | 8.3(3)           | 7669.6      | 39/2 <sup>-</sup> |
| 2122.9(2)        | 0.9(2)           | 7705.9      | 39/2 <sup>-</sup> |
| 2135.6(2)        | 0.7(2)           | 7718.4      | 39/2 <sup>-</sup> |
| 2185.7           | 1.7(3)           | 7768.5      | 39/2 <sup>-</sup> |
| 2217.2           | 1.7(3)           | 7800.3      | 39/2 <sup>-</sup> |

<sup>a</sup>Unobserved transition. The presence deduced from the coincidence analysis and  $\gamma$  intensity is calculated using the total transition intensity estimated in this analysis and multipolarity defined by spin-parity assignments of initial and final levels. The same holds for the 71.8 keV transition, which was observed but its  $\gamma$  intensity could not be accurately determined.

<sup>b</sup>Transitions used to normalize isomer decay intensity to 1000 units.

TABLE II. List of transitions for which the total electron conversion coefficients (TECC) could be determined from the intensity balance observed in the selected coincidence spectra. For most cases, values of the TECC listed in the second column uniquely assign the transition character indicated in the third column. For four transitions the TECC allowed  $M1$  or  $E2$  character, but  $M1$  assignment indicated in parentheses is strongly favored in observed decay. These results were used together with all other ones available from previous investigations to assign spin and parity values for the main levels populated in the isomer decay.

| $E_\gamma$<br>[keV] | $\alpha_{\text{tot}}$<br>experimental | Assigned<br>multipolarity | $\alpha_{\text{tot}}$<br>theoretical |
|---------------------|---------------------------------------|---------------------------|--------------------------------------|
| 68.0                | 5(2)                                  | $M1$                      | 6.1                                  |
| 72.7                | 6(2)                                  | $M1$                      | 5.05                                 |
| 73.7                | 5(3)                                  | $M1$                      | 4.9                                  |
| 80.4                | 4.1(5)                                | $M1$                      | 3.8                                  |
| 105.5               | 2.9(14)                               | ( $M1$ )                  | 1.7                                  |
| 110.0               | 1.9(5)                                | ( $M1$ )                  | 1.5                                  |
| 117.2               | 1.20(15)                              | $M1$                      | 1.28                                 |
| 120.2               | 1.05(18)                              | $M1$                      | 1.19                                 |
| 155.5               | 0.9(3)                                | $M1$                      | 0.58                                 |
| 157.5               | 0.6(2)                                | ( $M1$ )                  | 0.56                                 |
| 159.7               | 0.54(4)                               | $M1$                      | 0.53                                 |
| 168.2               | 0.6(3)                                | $M1$                      | 0.46                                 |
| 200.7               | 0.34(8)                               | $M1$                      | 0.28                                 |
| 204.4               | 0.22(6)                               | ( $M1$ )                  | 0.27                                 |
| 207.4               | 0.27(6)                               | $M1$                      | 0.26                                 |
| 207.7               | 0.38(15)                              | $M1$                      | 0.26                                 |
| 228.1               | 0.25(7)                               | $M1$                      | 0.199                                |
| 254.4               | 0.12(3)                               | $E2$                      | 0.10                                 |
| 285.4               | 0.10(3)                               | $M1$                      | 0.11                                 |
| 330.8               | 0.07(2)                               | $M1$                      | 0.078                                |
| 339.2               | <0.03                                 | $E1$                      | 0.012                                |
| 340.1               | 0.07(1)                               | $M1$                      | 0.069                                |
| 434.5               | <0.03                                 | $E2$                      | 0.02                                 |

Transparent presentation of the 49/2<sup>+</sup> isomer decay scheme established in the present work is given in Table III. It includes the list of all levels and transitions as they are observed in the decay order, starting with four isomeric transitions, which depopulate the 8587.7 keV,  $T_{1/2} = 510$  ns isomer down to the single 997.1 keV transition carrying the total decay intensity to the <sup>147</sup>Gd ground state. In Table III the energy and  $I^\pi$  assignment of each level is followed by the list of depopulating transitions with branching intensities including the electron conversion. This is explained together with other details in the Table III caption. Important numerical result is the intensity balance calculated for each level and listed in the last two columns of Table III. The observed equality of the summed total intensities of transitions feeding the level from above and those depopulating the level is rather satisfactory and proves that the decay established in the present investigation is very complete. Whereas the transition intensity uncertainties listed in Table I allow us to conclude that for few levels this intensity balance is not perfect; one cannot exclude that the picture is even more complex involving in those cases groups of transitions with intensities in the range of the 10<sup>-4</sup>/decay, which remained unobserved.

The construction of the level scheme displayed in Fig. 1 and Fig. 2 and presented in Table III is based on the detailed analysis of many  $\gamma$ -coincidence spectra, which established the placement of all transitions listed in Table I. In the following, only few examples will be selected to document important and nontrivial cases, which will be also discussed later in connection with the level structure considerations. In Fig. 3 the general feature of the isomeric decay is outlined by displaying high-energy range of  $\gamma$ -coincidence spectra obtained from the  $\gamma\gamma$  matrix preselected by requiring delayed coincidences with most intense transitions occurring in the 27/2<sup>-</sup> isomer decay. Spectra displayed in Figs. 3(a) and 3(b) were obtained with gates placed on 200.7 and 330.8 keV transitions, respectively, and the observed clearly different set of coincident transitions shows that the isomeric decay is essentially proceeding in two largely separated ways. The 200.7 keV  $\gamma$  transition depopulates the 5582.8 keV, yrast 35/2<sup>-</sup> level and represents 47% of the total isomer decay intensity carried by many transitions marked in Fig. 3(a), including the characteristic group of high-energy transitions above 1.8 MeV. It should be noted that only the most intense lines are indicated by energies and the 1903 keV line is an example of the weakest transition observed in the earlier study [18]. A very different group of lines is enhanced in the Fig. 3(b) spectrum, which was obtained with the gate placed on 330.8 keV  $\gamma$  transition depopulating the 4948.6 keV, 31/2<sup>+</sup> level and representing 25% of the total isomer decay intensity. Whereas many crosstalk transitions connecting both parts could be established, essentially one observes that the negative parity 35/2<sup>-</sup> level and positive parity 31/2<sup>+</sup> yrast levels are populated by a rather well-separated group of transitions.

The identification of the new  $M2$  branch in the 27/2<sup>-</sup> isomer decay is documented by the coincidence spectrum displayed in Fig. 4. In the  $\gamma\gamma\gamma$  coincidence cube sorted with broad prompt time window the first gate was placed on

TABLE III. Levels populated in the  $49/2^+$  isomer decay in  $^{147}\text{Gd}$ . In subsequent columns are listed: level energies with 0.1 keV accuracy, assigned spin-parities, depopulating transition energies with the observed depopulation branchings (BR), transition multipolarities, energies and spin-parities of the final levels. Numbers listed in the last two columns give the full population and depopulation intensity observed at each level. The total depopulation branchings (BR) were calculated using  $\gamma$ -transition intensities listed in Table 1 and theoretical electron conversion coefficients.

| $E_i$ (keV) | $J_i^\pi$ | $E_\gamma$ (keV) | $\text{BR}_\gamma$ | Multipolarity | $E_f$ (keV) | $J_f^\pi$ | Feed in | Feed out          |
|-------------|-----------|------------------|--------------------|---------------|-------------|-----------|---------|-------------------|
| 8587.7      | $49/2^+$  | 254.4            | 91.2               | $E2^a$        | 8333.3      | $45/2^+$  | 911.6   | 1000 <sup>c</sup> |
|             |           | 434.5            | 5.9                | $E2^a$        | 8153.4      | $45/2^+$  |         |                   |
|             |           | 593.7            | 2.8                | $E3^a$        | 7994.2      | $43/2^-$  |         |                   |
|             |           | 623.8            | 0.1                | $E3$          | 7963.8      | $43/2^-$  |         |                   |
| 8333.3      | $45/2^+$  | 179.8            | 0.2                | $M1$          | 8153.4      | $45/2^+$  | 911.6   | 921.2             |
|             |           | 207.4            | 4.1                | $M1^a$        | 8125.9      | $43/2^+$  |         |                   |
|             |           | 236.2            | 1.0                | $M1$          | 8097.1      | $43/2^+$  |         |                   |
|             |           | 339.2            | 86.0               | $E1^a$        | 7994.2      | $43/2^-$  |         |                   |
|             |           | 369.4            | 6.6                | $E1^a$        | 7963.8      | $43/2^-$  |         |                   |
|             |           | 561.6            | 0.3                | $M1$          | 7771.9      | $43/2^+$  |         |                   |
|             |           | 944.0            | 1.2                | $M1$          | 7389.3      | $43/2^+$  |         |                   |
|             |           | 1298.1           | 0.4                | $E2$          | 7035.2      | $41/2^+$  |         |                   |
|             |           | 1426.6           | 0.3                | $E2$          | 6906.7      | $41/2^+$  |         |                   |
| 8153.4      | $45/2^+$  | 381.5            | 8.3                | $M1$          | 7771.9      | $43/2^+$  | 61.0    | 66.4              |
|             |           | 764.1            | 84.5               | $M1^a$        | 7389.3      | $43/2^+$  |         |                   |
|             |           | 1118.1           | 7.2                | $E2$          | 7035.2      | $41/2^+$  |         |                   |
| 8125.9      | $43/2^+$  | 354.0            | 1.2                | $M1$          | 7771.9      | $43/2^+$  | 37.4    | 35.9              |
|             |           | 773.6            | 11.7               | $M1$          | 7352.4      | $41/2^+$  |         |                   |
|             |           | 913.3            | 6.2                | $E1$          | 7212.6      | $41/2^-$  |         |                   |
|             |           | 1090.7           | 44.3               | $M1$          | 7035.2      | $41/2^+$  |         |                   |
| 8097.1      | $43/2^+$  | 1219.2           | 36.6               | $M1$          | 6906.7      | $41/2^+$  | 9.6     | 9.5               |
|             |           | 884.7            | 9.3                | $E1$          | 7212.6      | $41/2^-$  |         |                   |
|             |           | 1061.9           | 68.6               | $M1$          | 7035.2      | $41/2^+$  |         |                   |
| 7994.2      | $43/2^-$  | 1190.2           | 22.1               | $M1$          | 6906.7      | $41/2^+$  | 820.2   | 826.0             |
|             |           | 30.4             | 8.8                | $M1^b$        | 7963.8      | $43/2^-$  |         |                   |
|             |           | 77.2             | 0.3                | $M1^b$        | 7917.0      | $41/2^-$  |         |                   |
|             |           | 90.8             | 0.4                | $M1$          | 7903.5      | $41/2^-$  |         |                   |
|             |           | 120.2            | 59.1               | $M1^a$        | 7873.9      | $41/2^-$  |         |                   |
|             |           | 168.6            | 4.7                | $M1$          | 7825.6      | $41/2^-$  |         |                   |
|             |           | 192.9            | 5.2                | $M1$          | 7801.3      | $41/2^-$  |         |                   |
|             |           | 193.9            | 0.0                | $E2$          | 7800.3      | $39/2^-$  |         |                   |
|             |           | 288.3            | 0.2                | $E2$          | 7705.9      | $39/2^-$  |         |                   |
|             |           | 302.4            | 0.1                | $E1$          | 7691.9      | $41/2^+$  |         |                   |
|             |           | 327.9            | 0.8                | $M1$          | 7666.2      | $41/2^-$  |         |                   |
|             |           | 374.5            | 0.4                | $E1$          | 7619.7      | $41/2^+$  |         |                   |
|             |           | 463.3            | 1.9                | $E1$          | 7530.8      | $41/2^+$  |         |                   |
|             |           | 598.2            | 2.3                | $E1$          | 7396.0      | $41/2^+$  |         |                   |
|             |           | 605.0            | 3.5                | $E1$          | 7389.3      | $43/2^+$  |         |                   |
|             |           | 641.8            | 0.3                | $E1$          | 7352.4      | $41/2^+$  |         |                   |
|             |           | 686.7            | 0.7                | $E2$          | 7307.5      | $39/2^-$  |         |                   |
| 781.7       | 1.9       | $M1$             | 7212.6             | $41/2^-$      |             |           |         |                   |
| 867.4       | 0.2       | $E2$             | 7126.6             | $39/2^-$      |             |           |         |                   |
| 958.9       | 4.8       | $E1^a$           | 7035.2             | $41/2^+$      |             |           |         |                   |
| 1087.4      | 4.4       | $E1$             | 6906.7             | $41/2^+$      |             |           |         |                   |
| 7963.8      | $43/2^-$  | 162.4            | 0.9                | $M1$          | 7801.3      | $41/2^-$  | 134.7   | 152.6             |
|             |           | 297.8            | 1.7                | $M1$          | 7666.2      | $41/2^-$  |         |                   |
|             |           | 344.0            | 1.4                | $E1$          | 7619.7      | $41/2^+$  |         |                   |
|             |           | 433.1            | 7.4                | $E1$          | 7530.8      | $41/2^+$  |         |                   |
|             |           | 567.9            | 3.7                | $E1$          | 7396.0      | $41/2^+$  |         |                   |
|             |           | 574.5            | 7.0                | $E1$          | 7389.3      | $43/2^+$  |         |                   |
|             |           | 656.3            | 1.6                | $E2$          | 7307.5      | $39/2^-$  |         |                   |
|             |           | 751.3            | 3.6                | $M1$          | 7212.6      | $41/2^-$  |         |                   |



TABLE III. (Continued.)

| $E_i$ (keV) | $J_i^\pi$ | $E_\gamma$ (keV) | $BR_\gamma$ | Multipolarity | $E_f$ (keV) | $J_f^\pi$ | Feed in | Feed out |
|-------------|-----------|------------------|-------------|---------------|-------------|-----------|---------|----------|
|             |           | 837.0            | 0.4         | $E2$          | 7126.6      | $39/2^-$  |         |          |
|             |           | 928.6            | 15.0        | $E1$          | 7035.2      | $41/2^+$  |         |          |
|             |           | 1057.1           | 57.3        | $E1^a$        | 6906.7      | $41/2^+$  |         |          |
| 7917.0      | $41/2^-$  | 247.3            | 37.9        | $M1$          | 7669.6      | $39/2^-$  | 2.1     | 3.4      |
|             |           | 1994.1           | 62.1        | $E2$          | 5922.9      | $37/2^-$  |         |          |
| 7903.5      | $41/2^-$  | 721.3            | 7.8         | $E1$          | 7182.7      | $39/2^+$  | 3.2     | 5.6      |
|             |           | 1065.0           | 19.6        | $E1$          | 6838.4      | $39/2^+$  |         |          |
|             |           | 1980.6           | 72.5        | $E2$          | 5922.9      | $37/2^-$  |         |          |
| 7873.9      | $41/2^-$  | 48.3             | 5.2         | $M1^b$        | 7825.6      | $41/2^-$  | 488.4   | 443.6    |
|             |           | 72.7             | 19.6        | $M1^a$        | 7801.3      | $41/2^-$  |         |          |
|             |           | 73.7             | 2.3         | $M1^a$        | 7800.3      | $39/2^-$  |         |          |
|             |           | 105.5            | 0.3         | $M1^a$        | 7768.5      | $39/2^-$  |         |          |
|             |           | 155.5            | 0.6         | $M1^a$        | 7718.4      | $39/2^-$  |         |          |
|             |           | 168.2            | 0.1         | $M1^a$        | 7705.9      | $39/2^-$  |         |          |
|             |           | 204.4            | 2.6         | $M1^a$        | 7669.6      | $39/2^-$  |         |          |
|             |           | 207.7            | 2.4         | $M1^a$        | 7666.2      | $41/2^-$  |         |          |
|             |           | 228.1            | 2.0         | $M1^a$        | 7645.8      | $39/2^-$  |         |          |
|             |           | 278.0            | 0.4         | $M1$          | 7596.0      | $39/2^-$  |         |          |
|             |           | 488.0            | 0.4         | $E2$          | 7386.0      | $37/2^-$  |         |          |
|             |           | 566.3            | 0.9         | $M1$          | 7307.5      | $39/2^-$  |         |          |
|             |           | 598.7            | 0.6         | $M1$          | 7275.5      | $41/2^-$  |         |          |
|             |           | 691.1            | 0.9         | $M1$          | 7182.7      | $39/2^+$  |         |          |
|             |           | 747.2            | 3.9         | $M1$          | 7126.6      | $39/2^-$  |         |          |
|             |           | 749.7            | 0.1         | $M1$          | 7124.2      | $39/2^-$  |         |          |
|             |           | 838.7            | 10.9        | $E1^a$        | 7035.2      | $41/2^+$  |         |          |
|             |           | 855.8            | 0.4         | $M1$          | 7018.0      | $39/2^-$  |         |          |
|             |           | 937.2            | 9.0         | $E1^a$        | 6936.7      | $39/2^+$  |         |          |
|             |           | 967.1            | 5.9         | $E1^a$        | 6906.7      | $41/2^+$  |         |          |
|             |           | 979.2            | 4.4         | $E1$          | 6894.5      | $39/2^+$  |         |          |
|             |           | 1035.4           | 1.6         | $E1$          | 6838.4      | $39/2^+$  |         |          |
|             |           | 1040.4           | 1.2         | $E2^a$        | 6833.7      | $37/2^-$  |         |          |
|             |           | 1215.7           | 0.2         | $M1$          | 6658.4      | $39/2^-$  |         |          |
|             |           | 1252.7           | 8.4         | $E1$          | 6621.2      | $39/2^+$  |         |          |
|             |           | 1951.1           | 15.3        | $E2^a$        | 5922.9      | $37/2^-$  |         |          |
| 7825.6      | $41/2^-$  | 119.8            | 2.6         | $M1$          | 7705.9      | $39/2^-$  | 62.2    | 64.3     |
|             |           | 229.7            | 9.2         | $M1$          | 7596.0      | $39/2^-$  |         |          |
|             |           | 517.8            | 5.0         | $M1$          | 7307.5      | $39/2^-$  |         |          |
|             |           | 550.3            | 3.8         | $M1$          | 7275.5      | $41/2^-$  |         |          |
|             |           | 699.0            | 1.9         | $M1$          | 7126.6      | $39/2^-$  |         |          |
|             |           | 701.1            | 1.2         | $M1$          | 7124.2      | $39/2^-$  |         |          |
|             |           | 790.3            | 34.0        | $E1$          | 7035.2      | $41/2^+$  |         |          |
|             |           | 888.7            | 4.3         | $E1$          | 6936.7      | $39/2^+$  |         |          |
|             |           | 919.0            | 2.9         | $E1$          | 6906.7      | $41/2^+$  |         |          |
|             |           | 987.3            | 1.5         | $E1$          | 6838.4      | $39/2^+$  |         |          |
|             |           | 1102.4           | 1.0         | $M1$          | 6723.0      | $39/2^-$  |         |          |
|             |           | 1167.9           | 4.5         | $M1$          | 6658.4      | $39/2^-$  |         |          |
|             |           | 1204.5           | 11.7        | $E1$          | 6621.2      | $39/2^+$  |         |          |
|             |           | 1354.0           | 2.4         | $M1$          | 6471.3      | $39/2^-$  |         |          |
|             |           | 1902.7           | 13.9        | $E2$          | 5922.9      | $37/2^-$  |         |          |
| 7801.3      | $41/2^-$  | 109.0            | 1.1         | $E1$          | 7691.9      | $41/2^+$  | 130.9   | 124.0    |
|             |           | 205.4            | 3.0         | $M1$          | 7596.0      | $39/2^-$  |         |          |
|             |           | 526.1            | 2.0         | $M1$          | 7275.5      | $41/2^-$  |         |          |
|             |           | 618.7            | 1.8         | $M1$          | 7182.7      | $39/2^+$  |         |          |
|             |           | 674.8            | 0.6         | $M1$          | 7126.6      | $39/2^-$  |         |          |
|             |           | 765.9            | 2.2         | $E1$          | 7035.2      | $41/2^+$  |         |          |
|             |           | 864.6            | 15.3        | $E1$          | 6936.7      | $39/2^+$  |         |          |

TABLE III. (*Continued.*)

| $E_i$ (keV) | $J_i^\pi$ | $E_\gamma$ (keV) | $BR_\gamma$ | Multipolarity | $E_f$ (keV) | $J_f^\pi$ | Feed in | Feed out |
|-------------|-----------|------------------|-------------|---------------|-------------|-----------|---------|----------|
|             |           | 894.6            | 11.3        | $E1$          | 6906.7      | $41/2^+$  |         |          |
|             |           | 906.7            | 17.4        | $E1$          | 6894.5      | $39/2^+$  |         |          |
|             |           | 962.9            | 2.5         | $E1$          | 6838.4      | $39/2^+$  |         |          |
|             |           | 967.6            | 4.5         | $E2$          | 6833.7      | $37/2^-$  |         |          |
|             |           | 1104.3           | 4.5         | $M2$          | 6697.1      | $37/2^+$  |         |          |
|             |           | 1180.2           | 33.8        | $E1$          | 6621.2      | $39/2^+$  |         |          |
| 7800.3      | $39/2^-$  | 1079.1           | 12.9        | $M1$          | 6721.0      | $37/2^-$  | 10.7    | 11.2     |
|             |           | 1329.0           | 9.9         | $M1$          | 6471.3      | $39/2^-$  |         |          |
|             |           | 1877.5           | 62.4        | $M1$          | 5922.9      | $37/2^-$  |         |          |
|             |           | 2217.2           | 14.9        | $E2$          | 5582.8      | $35/2^-$  |         |          |
| 7771.9      | $43/2^+$  | 419.7            | 12.0        | $M1$          | 7352.4      | $41/2^+$  | 8.4     | 10.5     |
|             |           | 736.6            | 76.5        | $M1$          | 7035.2      | $41/2^+$  |         |          |
|             |           | 865.2            | 11.5        | $M1$          | 6906.7      | $41/2^+$  |         |          |
| 7768.5      | $39/2^-$  | 2185.7           | 100.0       | $E2$          | 5582.8      | $35/2^-$  | 1.2     | 1.7      |
| 7718.4      | $39/2^-$  | 1402.7           | 40.0        | $E1$          | 6315.7      | $37/2^+$  | 2.4     | 2.2      |
|             |           | 1795.2           | 30.0        | $M1$          | 5922.9      | $37/2^-$  |         |          |
|             |           | 2135.6           | 30.0        | $E2$          | 5582.8      | $35/2^-$  |         |          |
| 7705.9      | $39/2^-$  | 1047.5           | 71.4        | $M1$          | 6658.4      | $39/2^-$  | 4.1     | 3.1      |
|             |           | 2122.9           | 28.6        | $E2$          | 5582.8      | $35/2^-$  |         |          |
| 7691.9      | $41/2^+$  | 384.5            | 15.2        | $E1$          | 7307.5      | $39/2^-$  | 1.9     | 3.6      |
|             |           | 797.5            | 30.3        | $M1$          | 6894.5      | $39/2^+$  |         |          |
|             |           | 1070.6           | 54.5        | $M1$          | 6621.2      | $39/2^+$  |         |          |
| 7669.6      | $39/2^-$  | 73.7             | 13.1        | $M1^a$        | 7596.0      | $39/2^-$  | 12.8    | 14.4     |
|             |           | 283.5            | 8.5         | $M1$          | 7386.0      | $37/2^-$  |         |          |
|             |           | 1011.4           | 6.1         | $M1$          | 6658.4      | $39/2^-$  |         |          |
|             |           | 1198.0           | 9.2         | $M1$          | 6471.3      | $39/2^-$  |         |          |
|             |           | 1709.8           | 5.4         | $E2$          | 5959.6      | $35/2^-$  |         |          |
|             |           | 2086.8           | 57.6        | $E2$          | 5582.8      | $35/2^-$  |         |          |
| 7666.2      | $41/2^-$  | 539.4            | 14.9        | $M1$          | 7126.6      | $39/2^-$  | 19.3    | 17.8     |
|             |           | 1007.8           | 5.0         | $M1$          | 6658.4      | $39/2^-$  |         |          |
|             |           | 1194.9           | 80.1        | $M1$          | 6471.3      | $39/2^-$  |         |          |
| 7645.8      | $39/2^-$  | 1723.0           | 11.7        | $M1$          | 5922.9      | $37/2^-$  | 8.7     | 6.6      |
|             |           | 2063.0           | 88.3        | $E2$          | 5582.8      | $35/2^-$  |         |          |
| 7619.7      | $41/2^+$  | 312.0            | 4.3         | $E1$          | 7307.5      | $39/2^-$  | 5.2     | 10.3     |
|             |           | 584.5            | 20.4        | $M1$          | 7035.2      | $41/2^+$  |         |          |
|             |           | 781.3            | 32.3        | $M1$          | 6838.4      | $39/2^+$  |         |          |
|             |           | 998.5            | 14.0        | $M1$          | 6621.2      | $39/2^+$  |         |          |
|             |           | 1155.8           | 29.0        | $E2$          | 6463.8      | $37/2^+$  |         |          |
| 7596.0      | $39/2^-$  | 560.9            | 11.8        | $E1$          | 7035.2      | $41/2^+$  | 13.4    | 10.3     |
|             |           | 702.6            | 7.5         | $E1$          | 6894.5      | $39/2^+$  |         |          |
|             |           | 762.7            | 16.1        | $M1$          | 6833.7      | $37/2^-$  |         |          |
|             |           | 1132.1           | 23.7        | $E1$          | 6463.8      | $37/2^+$  |         |          |
|             |           | 2013.0           | 40.9        | $E2$          | 5582.8      | $35/2^-$  |         |          |
| 7530.8      | $41/2^+$  | 512.7            | 6.6         | $E1$          | 7018.0      | $39/2^-$  | 27.0    | 26.8     |
|             |           | 636.3            | 30.0        | $M1$          | 6894.5      | $39/2^+$  |         |          |
|             |           | 692.3            | 31.3        | $M1$          | 6838.4      | $39/2^+$  |         |          |
|             |           | 909.6            | 32.1        | $M1$          | 6621.2      | $39/2^+$  |         |          |
| 7396.0      | $41/2^+$  | 459.5            | 9.0         | $M1$          | 6936.7      | $39/2^+$  | 24.7    | 25.4     |
|             |           | 501.5            | 19.1        | $M1$          | 6894.5      | $39/2^+$  |         |          |
|             |           | 557.6            | 12.2        | $M1$          | 6838.4      | $39/2^+$  |         |          |
|             |           | 675.0            | 2.7         | $M2$          | 6721.0      | $37/2^-$  |         |          |
|             |           | 698.8            | 11.3        | $E2$          | 6697.1      | $37/2^+$  |         |          |
|             |           | 738.0            | 5.7         | $E1$          | 6658.4      | $39/2^-$  |         |          |
|             |           | 924.7            | 36.1        | $E1$          | 6471.3      | $39/2^-$  |         |          |
|             |           | 1080.5           | 3.9         | $E2$          | 6315.7      | $37/2^+$  |         |          |

TABLE III. (Continued.)

| $E_i$ (keV) | $J_i^\pi$         | $E_\gamma$ (keV) | $BR_\gamma$       | Multipolarity | $E_f$ (keV)       | $J_f^\pi$         | Feed in | Feed out |
|-------------|-------------------|------------------|-------------------|---------------|-------------------|-------------------|---------|----------|
| 7389.3      | 43/2 <sup>+</sup> | 177.0            | 1.9               | $E1$          | 7212.6            | 41/2 <sup>-</sup> | 106.9   | 113.7    |
|             |                   | 354.0            | 7.4               | $M1$          | 7035.2            | 41/2 <sup>+</sup> |         |          |
|             |                   | 482.6            | 89.9              | $M1^a$        | 6906.7            | 41/2 <sup>+</sup> |         |          |
|             |                   | 768.3            | 0.8               | $E2$          | 6621.2            | 39/2 <sup>+</sup> |         |          |
| 7386.0      | 37/2 <sup>-</sup> | 1803.2           | 84.4              | $M1$          | 5582.8            | 35/2 <sup>-</sup> | 3.1     | 3.5      |
|             |                   | 2004.2           | 15.6              | $E2$          | 5382.1            | 33/2 <sup>-</sup> |         |          |
| 7352.4      | 41/2 <sup>+</sup> | 514.0            | 100.0             | $M1$          | 6838.4            | 39/2 <sup>+</sup> | 8.1     | 6.2      |
| 7307.5      | 39/2 <sup>-</sup> | 739.8            | 5.2               | $E1$          | 6567.7            | 37/2 <sup>+</sup> | 16.2    | 17.0     |
|             |                   | 843.5            | 7.8               | $E1$          | 6463.8            | 37/2 <sup>+</sup> |         |          |
|             |                   | 991.8            | 87.0              | $E1$          | 6315.7            | 37/2 <sup>+</sup> |         |          |
| 7275.5      | 41/2 <sup>-</sup> | 1352.6           | 100.0             | $E2$          | 5922.9            | 37/2 <sup>-</sup> | 7.6     | 5.9      |
| 7212.6      | 41/2 <sup>-</sup> | 317.8            | 12.4              | $E1$          | 6894.5            | 39/2 <sup>+</sup> | 26.5    | 28.5     |
|             |                   | 374.2            | 36.8              | $E1$          | 6838.4            | 39/2 <sup>+</sup> |         |          |
|             |                   | 741.3            | 50.8              | $M1$          | 6471.3            | 39/2 <sup>-</sup> |         |          |
| 7182.7      | 39/2 <sup>+</sup> | 809.6            | 21.7              | $E1$          | 6373.2            | 37/2 <sup>-</sup> | 6.8     | 10.2     |
|             |                   | 860.7            | 7.6               | $E2$          | 6322.0            | 35/2 <sup>+</sup> |         |          |
|             |                   | 867.0            | 70.7              | $M1$          | 6315.7            | 37/2 <sup>+</sup> |         |          |
| 7126.6      | 39/2 <sup>-</sup> | 403.5            | 20.5              | $M1$          | 6723.0            | 39/2 <sup>-</sup> | 24.5    | 21.0     |
|             |                   | 1203.7           | 79.5              | $M1$          | 5922.9            | 37/2 <sup>-</sup> |         |          |
| 7124.2      | 39/2 <sup>-</sup> | 660.4            | 100.0             | $E1$          | 6463.8            | 37/2 <sup>+</sup> | 1.4     | 1.8      |
| 7035.2      | 41/2 <sup>+</sup> | 140.6            | 1.6               | $M1$          | 6894.5            | 39/2 <sup>+</sup> | 186.5   | 175.8    |
|             |                   | 196.6            | 3.8               | $M1$          | 6838.4            | 39/2 <sup>+</sup> |         |          |
|             |                   | 414.0            | 86.3              | $M1^a$        | 6621.2            | 39/2 <sup>+</sup> |         |          |
|             |                   | 571.5            | 6.0               | $E2$          | 6463.8            | 37/2 <sup>+</sup> |         |          |
|             |                   | 719.4            | 2.3               | $E2$          | 6315.7            | 37/2 <sup>+</sup> |         |          |
| 7018.0      | 39/2 <sup>-</sup> | 1095.1           | 100.0             | $M1$          | 5922.9            | 37/2 <sup>-</sup> | 3.8     | 3.2      |
| 6936.7      | 39/2 <sup>+</sup> | 239.6            | 19.9              | $M1$          | 6697.1            | 37/2 <sup>+</sup> | 64.0    | 60.4     |
|             |                   | 369.0            | 52.8              | $M1$          | 6567.7            | 37/2 <sup>+</sup> |         |          |
|             |                   | 465.4            | 9.2               | $E1$          | 6471.3            | 39/2 <sup>-</sup> |         |          |
|             |                   | 472.7            | 0.5               | $M1$          | 6463.8            | 37/2 <sup>+</sup> |         |          |
|             |                   | 620.9            | 2.6               | $M1$          | 6315.7            | 37/2 <sup>+</sup> |         |          |
|             |                   | 924.1            | 11.7              | $E2$          | 6012.8            | 35/2 <sup>+</sup> |         |          |
|             |                   | 1013.8           | 3.3               | $E1$          | 5922.9            | 37/2 <sup>-</sup> |         |          |
|             |                   | 6906.7           | 41/2 <sup>+</sup> | 12.1          | 1.3               | $M1^b$            |         |          |
| 68.0        | 1.4               | $M1^a$           |                   | 6838.4        | 39/2 <sup>+</sup> |                   |         |          |
| 248.4       | 1.8               | $E1$             |                   | 6658.4        | 39/2 <sup>-</sup> |                   |         |          |
| 285.4       | 42.1              | $M1^a$           |                   | 6621.2        | 39/2 <sup>+</sup> |                   |         |          |
| 435.3       | 42.3              | $E1^a$           |                   | 6471.3        | 39/2 <sup>-</sup> |                   |         |          |
| 6894.5      | 39/2 <sup>+</sup> | 591.1            | 11.0              | $E2^a$        | 6315.7            | 37/2 <sup>+</sup> | 66.2    | 64.1     |
|             |                   | 173.4            | 2.2               | $E1$          | 6721.0            | 37/2 <sup>-</sup> |         |          |
|             |                   | 326.8            | 10.0              | $M1$          | 6567.7            | 37/2 <sup>+</sup> |         |          |
|             |                   | 423.2            | 8.4               | $E1$          | 6471.3            | 39/2 <sup>-</sup> |         |          |
|             |                   | 430.8            | 3.9               | $M1$          | 6463.8            | 37/2 <sup>+</sup> |         |          |
|             |                   | 578.7            | 3.1               | $M1$          | 6315.7            | 37/2 <sup>+</sup> |         |          |
|             |                   | 971.6            | 72.3              | $E1^a$        | 5922.9            | 37/2 <sup>-</sup> |         |          |
| 6838.4      | 39/2 <sup>+</sup> | 374.8            | 13.4              | $M1$          | 6463.8            | 37/2 <sup>+</sup> | 54.6    | 46.9     |
|             |                   | 915.5            | 86.6              | $E1^a$        | 5922.9            | 37/2 <sup>-</sup> |         |          |
| 6833.7      | 37/2 <sup>-</sup> | 518.1            | 21.3              | $E1$          | 6315.7            | 37/2 <sup>+</sup> | 12.7    | 13.5     |
|             |                   | 820.8            | 61.5              | $E1$          | 6012.8            | 35/2 <sup>+</sup> |         |          |
|             |                   | 1250.5           | 17.2              | $M1$          | 5582.8            | 35/2 <sup>-</sup> |         |          |
| 6723.0      | 39/2 <sup>-</sup> | 800.1            | 21.7              | $M1$          | 5922.9            | 37/2 <sup>-</sup> | 5.0     | 5.1      |
|             |                   | 1140.2           | 78.3              | $E2$          | 5582.8            | 35/2 <sup>-</sup> |         |          |
| 6721.0      | 37/2 <sup>-</sup> | 798.0            | 28.8              | $M1$          | 5922.9            | 37/2 <sup>-</sup> | 3.5     | 5.7      |
|             |                   | 1138.2           | 71.2              | $M1$          | 5582.8            | 35/2 <sup>-</sup> |         |          |

TABLE III. (*Continued.*)

| $E_i$ (keV) | $J_i^\pi$ | $E_\gamma$ (keV) | $BR_\gamma$ | Multipolarity | $E_f$ (keV) | $J_f^\pi$ | Feed in | Feed out |
|-------------|-----------|------------------|-------------|---------------|-------------|-----------|---------|----------|
| 6697.1      | $37/2^+$  | 375.0            | 5.4         | $M1$          | 6322.0      | $35/2^+$  | 20.4    | 17.0     |
|             |           | 929.8            | 36.3        | $E1$          | 5767.3      | $35/2^-$  |         |          |
|             |           | 1114.3           | 49.2        | $E1$          | 5582.8      | $35/2^-$  |         |          |
|             |           | 1668.2           | 9.1         | $E2$          | 5029.0      | $33/2^+$  |         |          |
| 6658.4      | $39/2^-$  | 285.2            | 51.1        | $M1$          | 6373.2      | $37/2^-$  | 14.9    | 10.4     |
|             |           | 576.9            | 17.0        | $E2$          | 6081.4      | $35/2^-$  |         |          |
|             |           | 698.9            | 31.9        | $E2$          | 5959.6      | $35/2^-$  |         |          |
| 6621.2      | $39/2^+$  | 157.5            | 6.2         | $M1^a$        | 6463.8      | $37/2^+$  | 377.6   | 366.6    |
|             |           | 248.1            | 1.1         | $E1$          | 6373.2      | $37/2^-$  |         |          |
|             |           | 299.1            | 1.9         | $E2$          | 6322.0      | $35/2^+$  |         |          |
|             |           | 440.1            | 0.7         | $E2$          | 6181.3      | $35/2^+$  |         |          |
|             |           | 608.5            | 38.0        | $E2^a$        | 6012.8      | $35/2^+$  |         |          |
|             |           | 698.3            | 51.0        | $E1^a$        | 5922.9      | $37/2^-$  |         |          |
|             |           | 853.9            | 0.3         | $M2$          | 5767.3      | $35/2^-$  |         |          |
|             |           | 1038.3           | 0.9         | $M2$          | 5582.8      | $35/2^-$  |         |          |
| 6567.7      | $37/2^+$  | 554.8            | 2.1         | $M1$          | 6012.8      | $35/2^+$  | 39.2    | 36.1     |
|             |           | 645.0            | 12.8        | $E1$          | 5922.9      | $37/2^-$  |         |          |
|             |           | 800.5            | 6.4         | $E1$          | 5767.3      | $35/2^-$  |         |          |
|             |           | 984.8            | 70.3        | $E1^a$        | 5582.8      | $35/2^-$  |         |          |
|             |           | 1538.8           | 8.3         | $E2$          | 5029.0      | $33/2^+$  |         |          |
| 6471.3      | $39/2^-$  | 155.5            | 0.4         | $E1$          | 6315.7      | $37/2^+$  | 179.4   | 169.6    |
|             |           | 548.4            | 94.3        | $M1^a$        | 5922.9      | $37/2^-$  |         |          |
|             |           | 703.9            | 2.0         | $E2$          | 5767.3      | $35/2^-$  |         |          |
|             |           | 888.5            | 3.3         | $E2$          | 5582.8      | $35/2^-$  |         |          |
| 6463.8      | $37/2^+$  | 282.6            | 16.8        | $M1$          | 6181.3      | $35/2^+$  | 50.8    | 49.3     |
|             |           | 382.8            | 1.8         | $E1$          | 6081.4      | $35/2^-$  |         |          |
|             |           | 504.6            | 4.0         | $E1$          | 5959.6      | $35/2^-$  |         |          |
|             |           | 696.5            | 10.1        | $E1$          | 5767.3      | $35/2^-$  |         |          |
|             |           | 880.8            | 8.5         | $E1$          | 5582.8      | $35/2^-$  |         |          |
|             |           | 1434.7           | 58.8        | $E2^a$        | 5029.0      | $33/2^+$  |         |          |
| 6373.2      | $37/2^-$  | 192.2            | 5.6         | $E1$          | 6181.3      | $35/2^+$  | 11.5    | 17.9     |
|             |           | 291.9            | 6.1         | $M1$          | 6081.4      | $35/2^-$  |         |          |
|             |           | 413.7            | 16.1        | $M1$          | 5959.6      | $35/2^-$  |         |          |
|             |           | 605.8            | 22.6        | $M1$          | 5767.3      | $35/2^-$  |         |          |
|             |           | 790.3            | 49.7        | $M1$          | 5582.8      | $35/2^-$  |         |          |
| 6322.0      | $35/2^+$  | 700.0            | 22.1        | $E1$          | 5622.1      | $33/2^+$  | 8.8     | 7.5      |
|             |           | 1293.0           | 57.4        | $M1$          | 5029.0      | $33/2^+$  |         |          |
|             |           | 1373.5           | 20.6        | $E2$          | 4948.6      | $31/2^+$  |         |          |
| 6315.7      | $37/2^+$  | 303.1            | 4.5         | $M1$          | 6012.8      | $35/2^+$  | 67.8    | 67.0     |
|             |           | 548.5            | 9.3         | $E1$          | 5767.3      | $35/2^-$  |         |          |
|             |           | 733.2            | 4.1         | $E1$          | 5582.8      | $35/2^-$  |         |          |
|             |           | 1286.7           | 82.1        | $E2^a$        | 5029.0      | $33/2^+$  |         |          |
| 6181.3      | $35/2^+$  | 168.6            | 12.8        | $M1$          | 6012.8      | $35/2^+$  | 11.8    | 15.1     |
|             |           | 410.4            | 5.9         | $E1$          | 5771.0      | $33/2^-$  |         |          |
|             |           | 559.1            | 11.0        | $M1$          | 5622.1      | $33/2^+$  |         |          |
|             |           | 1152.1           | 19.8        | $M1$          | 5029.0      | $33/2^+$  |         |          |
|             |           | 1232.7           | 50.5        | $E2$          | 4948.6      | $31/2^+$  |         |          |
| 6081.4      | $35/2^-$  | 428.7            | 14.6        | $M1$          | 5652.6      | $33/2^-$  | 3.7     | 10.6     |
|             |           | 642.5            | 12.5        | $E2$          | 5439.3      | $31/2^-$  |         |          |
|             |           | 699.0            | 10.4        | $M1$          | 5382.1      | $33/2^-$  |         |          |
|             |           | 1109.7           | 12.5        | $E2$          | 4971.7      | $31/2^-$  |         |          |
|             |           | 1237.6           | 50.0        | $E2$          | 4843.7      | $31/2^-$  |         |          |
| 6012.8      | $35/2^+$  | 245.8            | 0.4         | $E1$          | 5767.3      | $35/2^-$  | 160.2   | 151.4    |
|             |           | 270.4            | 12.2        | $M1$          | 5742.2      | $33/2^+$  |         |          |
|             |           | 360.2            | 9.4         | $E1$          | 5652.6      | $33/2^-$  |         |          |
|             |           | 390.5            | 5.2         | $M1$          | 5622.1      | $33/2^+$  |         |          |

TABLE III. (Continued.)

| $E_i$ (keV) | $J_i^\pi$ | $E_\gamma$ (keV) | $BR_\gamma$ | Multipolarity | $E_f$ (keV) | $J_f^\pi$ | Feed in | Feed out |
|-------------|-----------|------------------|-------------|---------------|-------------|-----------|---------|----------|
|             |           | 430.0            | 0.3         | $E1$          | 5582.8      | $35/2^-$  |         |          |
|             |           | 630.7            | 1.2         | $E1$          | 5382.1      | $33/2^-$  |         |          |
|             |           | 983.8            | 34.1        | $M1^a$        | 5029.0      | $33/2^+$  |         |          |
|             |           | 1064.3           | 37.3        | $E2^a$        | 4948.6      | $31/2^+$  |         |          |
| 5959.6      | $35/2^-$  | 306.9            | 37.3        | $M1$          | 5652.6      | $33/2^-$  | 8.9     | 5.8      |
|             |           | 520.4            | 62.7        | $E2$          | 5439.3      | $31/2^-$  |         |          |
| 5922.9      | $37/2^-$  | 340.1            | 95.1        | $M1^a$        | 5582.8      | $35/2^-$  | 560.4   | 577.0    |
|             |           | 540.9            | 4.9         | $E2$          | 5382.1      | $33/2^-$  |         |          |
| 5771.0      | $33/2^-$  | 799.3            | 100.0       | $E1$          | 4971.7      | $31/2^-$  | 0.9     | 2.3      |
| 5767.3      | $35/2^-$  | 385.4            | 16.7        | $M1$          | 5382.1      | $33/2^-$  | 28.8    | 27.8     |
|             |           | 738.2            | 39.7        | $E1$          | 5029.0      | $33/2^+$  |         |          |
|             |           | 795.7            | 37.7        | $E2$          | 4971.7      | $31/2^-$  |         |          |
|             |           | 923.8            | 6.0         | $E2$          | 4843.7      | $31/2^-$  |         |          |
| 5742.2      | $33/2^+$  | 470.0            | 18.5        | $E1$          | 5272.1      | $31/2^-$  | 18.4    | 22.8     |
|             |           | 713.4            | 7.3         | $M1$          | 5029.0      | $33/2^+$  |         |          |
|             |           | 770.7            | 4.8         | $E1$          | 4971.7      | $31/2^-$  |         |          |
|             |           | 793.8            | 4.8         | $M1$          | 4948.6      | $31/2^+$  |         |          |
|             |           | 898.3            | 14.5        | $E1$          | 4843.7      | $31/2^-$  |         |          |
|             |           | 1124.4           | 49.9        | $E2$          | 4617.8      | $29/2^+$  |         |          |
| 5652.6      | $33/2^-$  | 213.3            | 6.2         | $M1$          | 5439.3      | $31/2^-$  | 18.0    | 19.5     |
|             |           | 623.4            | 4.0         | $E1$          | 5029.0      | $33/2^+$  |         |          |
|             |           | 680.8            | 16.9        | $M1$          | 4971.7      | $31/2^-$  |         |          |
|             |           | 704.0            | 10.2        | $E1$          | 4948.6      | $31/2^+$  |         |          |
|             |           | 808.8            | 7.3         | $M1$          | 4843.7      | $31/2^-$  |         |          |
|             |           | 1422.8           | 55.4        | $E2$          | 4229.8      | $29/2^-$  |         |          |
| 5622.1      | $33/2^+$  | 350.0            | 33.9        | $E1$          | 5272.1      | $31/2^-$  | 11.2    | 10.5     |
|             |           | 593.0            | 9.6         | $M1$          | 5029.0      | $33/2^+$  |         |          |
|             |           | 650.4            | 4.2         | $E1$          | 4971.7      | $31/2^-$  |         |          |
|             |           | 673.6            | 29.3        | $M1$          | 4948.6      | $31/2^+$  |         |          |
|             |           | 778.4            | 23.0        | $E1$          | 4843.7      | $31/2^-$  |         |          |
| 5582.8      | $35/2^-$  | 200.7            | 89.5        | $M1^a$        | 5382.1      | $33/2^-$  | 644.4   | 675.1    |
|             |           | 317.9            | 1.5         | $E2$          | 5264.9      | $31/2^-$  |         |          |
|             |           | 553.9            | 0.6         | $E1$          | 5029.0      | $33/2^+$  |         |          |
|             |           | 611.4            | 8.5         | $E2^a$        | 4971.7      | $31/2^-$  |         |          |
| 5439.3      | $31/2^-$  | 906.0            | 13.6        | $M1$          | 4533.5      | $29/2^-$  | 6.2     | 6.5      |
|             |           | 1857.6           | 86.4        | $E2$          | 3581.7      | $27/2^-$  |         |          |
| 5382.1      | $33/2^-$  | 117.2            | 62.1        | $M1^a$        | 5264.9      | $31/2^-$  | 640.2   | 652.7    |
|             |           | 264.0            | 0.4         | $M1$          | 5117.9      | $29/2^-$  |         |          |
|             |           | 352.9            | 4.1         | $E1$          | 5029.0      | $33/2^+$  |         |          |
|             |           | 410.4            | 3.8         | $M1$          | 4971.7      | $31/2^-$  |         |          |
|             |           | 433.6            | 1.3         | $E1$          | 4948.6      | $31/2^+$  |         |          |
|             |           | 538.4            | 6.6         | $M1$          | 4843.7      | $31/2^-$  |         |          |
|             |           | 848.7            | 6.7         | $E2$          | 4533.5      | $29/2^-$  |         |          |
|             |           | 1152.2           | 15.1        | $E2^a$        | 4229.8      | $29/2^-$  |         |          |
| 5272.1      | $31/2^-$  | 654.4            | 55.1        | $E1$          | 4617.8      | $29/2^+$  | 7.8     | 10.8     |
|             |           | 821.4            | 44.9        | $M1$          | 4450.6      | $29/2^-$  |         |          |
| 5264.9      | $31/2^-$  | 146.8            | 1.1         | $M1$          | 5117.9      | $29/2^-$  | 415.1   | 427.3    |
|             |           | 236.1            | 0.6         | $E1$          | 5029.0      | $33/2^+$  |         |          |
|             |           | 293.0            | 0.3         | $M1$          | 4971.7      | $31/2^-$  |         |          |
|             |           | 316.0            | 1.1         | $E1$          | 4948.6      | $31/2^+$  |         |          |
|             |           | 421.2            | 18.0        | $M1^a$        | 4843.7      | $31/2^-$  |         |          |
|             |           | 647.2            | 1.4         | $E1$          | 4617.8      | $29/2^+$  |         |          |
|             |           | 814.2            | 18.5        | $M1^a$        | 4450.6      | $29/2^-$  |         |          |
|             |           | 927.2            | 2.0         | $E2$          | 4338.0      | $27/2^-$  |         |          |
|             |           | 1053.6           | 1.7         | $E2$          | 4211.4      | $27/2^-$  |         |          |
|             |           | 1195.0           | 2.5         | $E2$          | 4070.1      | $27/2^-$  |         |          |

TABLE III. (*Continued.*)

| $E_i$ (keV) | $J_i^\pi$ | $E_\gamma$ (keV) | $BR_\gamma$ | Multipolarity | $E_f$ (keV) | $J_f^\pi$ | Feed in | Feed out |
|-------------|-----------|------------------|-------------|---------------|-------------|-----------|---------|----------|
|             |           | 1258.2           | 1.9         | $E2$          | 4006.6      | $27/2^-$  |         |          |
|             |           | 1683.3           | 50.9        | $E2^a$        | 3581.7      | $27/2^-$  |         |          |
| 5117.9      | $29/2^-$  | 1426.1           | 32.1        | $E2$          | 3691.7      | $25/2^-$  | 7.3     | 8.6      |
|             |           | 1536.2           | 67.9        | $M1$          | 3581.7      | $27/2^-$  |         |          |
| 5029.0      | $33/2^+$  | 57.4             | 1.6         | $E1$          | 4971.7      | $31/2^-$  | 194.9   | 216.7    |
|             |           | 80.4             | 95.3        | $M1^a$        | 4948.6      | $31/2^+$  |         |          |
|             |           | 185.2            | 3.1         | $E1$          | 4843.7      | $31/2^-$  |         |          |
| 4971.7      | $31/2^-$  | 520.9            | 3.7         | $M1$          | 4450.6      | $29/2^-$  | 105.7   | 111.3    |
|             |           | 742.0            | 5.9         | $M1$          | 4229.8      | $29/2^-$  |         |          |
|             |           | 964.9            | 3.6         | $E2$          | 4006.6      | $27/2^-$  |         |          |
|             |           | 1390.0           | 86.9        | $E2^a$        | 3581.7      | $27/2^-$  |         |          |
| 4948.6      | $31/2^+$  | 330.8            | 88.9        | $M1^a$        | 4617.8      | $29/2^+$  | 291.4   | 297.1    |
|             |           | 415.2            | 3.0         | $E1$          | 4533.5      | $29/2^-$  |         |          |
|             |           | 498.0            | 8.0         | $E1$          | 4450.6      | $29/2^-$  |         |          |
| 4843.7      | $31/2^-$  | 310.2            | 0.9         | $M1$          | 4533.5      | $29/2^-$  | 140.6   | 131.3    |
|             |           | 393.1            | 24.4        | $M1$          | 4450.6      | $29/2^-$  |         |          |
|             |           | 614.0            | 38.4        | $M1^a$        | 4229.8      | $29/2^-$  |         |          |
|             |           | 836.7            | 4.3         | $E2$          | 4006.6      | $27/2^-$  |         |          |
|             |           | 1261.9           | 32.0        | $E2^a$        | 3581.7      | $27/2^-$  |         |          |
| 4617.8      | $29/2^+$  | 279.6            | 0.2         | $E1$          | 4338.0      | $27/2^-$  | 287.6   | 272.1    |
|             |           | 406.5            | 2.2         | $E1$          | 4211.4      | $27/2^-$  |         |          |
|             |           | 611.2            | 6.7         | $E1$          | 4006.6      | $27/2^-$  |         |          |
|             |           | 1036.1           | 90.2        | $E1^a$        | 3581.7      | $27/2^-$  |         |          |
|             |           | 1219.1           | 0.7         | $E2$          | 3398.8      | $25/2^+$  |         |          |
| 4533.5      | $29/2^-$  | 303.5            | 5.1         | $M1$          | 4229.8      | $29/2^-$  | 55.1    | 58.4     |
|             |           | 322.1            | 9.2         | $M1$          | 4211.4      | $27/2^-$  |         |          |
|             |           | 463.4            | 50.6        | $M1$          | 4070.1      | $27/2^-$  |         |          |
|             |           | 526.8            | 16.0        | $M1$          | 4006.6      | $27/2^-$  |         |          |
|             |           | 951.7            | 19.1        | $M1$          | 3581.7      | $27/2^-$  |         |          |
| 4450.6      | $29/2^-$  | 380.7            | 1.8         | $M1$          | 4070.1      | $27/2^-$  | 143.9   | 147.4    |
|             |           | 444.0            | 36.3        | $M1^a$        | 4006.6      | $27/2^-$  |         |          |
|             |           | 759.1            | 3.3         | $E2$          | 3691.7      | $25/2^-$  |         |          |
|             |           | 868.9            | 58.6        | $M1^a$        | 3581.7      | $27/2^-$  |         |          |
| 4338.0      | $27/2^-$  | 646.2            | 35.0        | $M1$          | 3691.7      | $25/2^-$  | 9.2     | 8.5      |
|             |           | 756.2            | 19.6        | $M1$          | 3581.7      | $27/2^-$  |         |          |
|             |           | 939.3            | 45.4        | $E1$          | 3398.8      | $25/2^+$  |         |          |
| 4229.8      | $29/2^-$  | 159.7            | 76.8        | $M1^a$        | 4070.1      | $27/2^-$  | 169.2   | 160.1    |
|             |           | 223.0            | 20.3        | $M1$          | 4006.6      | $27/2^-$  |         |          |
|             |           | 647.9            | 2.9         | $M1$          | 3581.7      | $27/2^-$  |         |          |
| 4211.4      | $27/2^-$  | 519.5            | 23.0        | $M1$          | 3691.7      | $25/2^-$  | 18.6    | 18.2     |
|             |           | 812.6            | 77.0        | $E1$          | 3398.8      | $25/2^+$  |         |          |
| 4070.1      | $27/2^-$  | 378.4            | 80.3        | $M1^a$        | 3691.7      | $25/2^-$  | 166.0   | 150.4    |
|             |           | 488.4            | 3.5         | $M1$          | 3581.7      | $27/2^-$  |         |          |
|             |           | 671.4            | 16.2        | $E1$          | 3398.8      | $25/2^+$  |         |          |
| 4006.6      | $27/2^-$  | 315.0            | 19.7        | $M1$          | 3691.7      | $25/2^-$  | 131.4   | 134.4    |
|             |           | 424.9            | 80.3        | $M1^a$        | 3581.7      | $27/2^-$  |         |          |
| 3691.7      | $25/2^-$  | 110.0            | 42.0        | $M1^a$        | 3581.7      | $27/2^-$  | 162.0   | 159.6    |
|             |           | 181.8            | 10.4        | $M1$          | 3510.0      | $23/2^-$  |         |          |
|             |           | 293.0            | 3.2         | $E1$          | 3398.8      | $25/2^+$  |         |          |
|             |           | 505.5            | 13.3        | $E1^a$        | 3186.1      | $23/2^+$  |         |          |
|             |           | 653.8            | 31.1        | $E1^a$        | 3038.0      | $23/2^+$  |         |          |
| 3581.7      | $27/2^-$  | 71.8             | 1.1         | $E2$          | 3510.0      | $23/2^-$  | 897.2   | 900.5    |
|             |           | 182.9            | 78.7        | $E1^a$        | 3398.8      | $25/2^+$  |         |          |
|             |           | 395.5            | 1.6         | $M2$          | 3186.1      | $23/2^+$  |         |          |
|             |           | 543.7            | 13.9        | $M2^a$        | 3038.0      | $23/2^+$  |         |          |
|             |           | 821.3            | 4.6         | $E3^a$        | 2760.2      | $21/2^+$  |         |          |

TABLE III. (Continued.)

| $E_i$ (keV) | $J_i^\pi$ | $E_\gamma$ (keV) | $BR_\gamma$ | Multipolarity | $E_f$ (keV) | $J_f^\pi$ | Feed in | Feed out          |
|-------------|-----------|------------------|-------------|---------------|-------------|-----------|---------|-------------------|
| 3510.0      | $23/2^-$  | 323.8            | 4.9         | $E1$          | 3186.1      | $23/2^+$  | 26.8    | 29.0              |
|             |           | 471.9            | 13.0        | $E1$          | 3038.0      | $23/2^+$  |         |                   |
|             |           | 749.7            | 19.1        | $E1$          | 2760.2      | $21/2^+$  |         |                   |
|             |           | 937.9            | 63.0        | $E2$          | 2572.1      | $19/2^-$  |         |                   |
| 3398.8      | $25/2^+$  | 212.6            | 0.2         | $M1$          | 3186.1      | $23/2^+$  | 758.2   | 781.5             |
|             |           | 360.8            | 92.8        | $M1^a$        | 3038.0      | $23/2^+$  |         |                   |
|             |           | 638.6            | 7.0         | $E2^a$        | 2760.2      | $21/2^+$  |         |                   |
| 3186.1      | $23/2^+$  | 425.9            | 100.0       | $M1^a$        | 2760.2      | $21/2^+$  | 39.0    | 34.4              |
| 3038.0      | $23/2^+$  | 277.8            | 100.0       | $M1^a$        | 2760.2      | $21/2^+$  | 903.6   | 888.7             |
| 2760.2      | $21/2^+$  | 188.1            | 16.4        | $E1^a$        | 2572.1      | $19/2^-$  | 1025.0  | 992.2             |
|             |           | 272.1            | 83.6        | $E2^a$        | 2488.1      | $17/2^+$  |         |                   |
| 2572.1      | $19/2^-$  | 83.9             | 50.0        | $E1^a$        | 2488.1      | $17/2^+$  | 181.0   | 185.6             |
|             |           | 1575.1           | 50.0        | $E3^a$        | 997.1       | $13/2^+$  |         |                   |
|             |           | 2488.1           | 100.0       | $E2^a$        | 997.1       | $13/2^+$  |         |                   |
| 997.1       | $13/2^+$  | 997.1            | 100.0       | $E3^a$        | 0.0         | $7/2^-$   | 998.0   | 1000 <sup>c</sup> |
| 0.0         | $7/2^-$   |                  |             |               |             |           | 1000    |                   |

<sup>a</sup>Assigned on the basis of current (Table II) and previous works [18,19].

<sup>b</sup>Unobserved transition, see remark in Table 1.

<sup>c</sup>Used to normalize.

the 425.9 keV transition depopulating the 3186.1 keV level and the second gates were placed on the four most intense transitions feeding the  $27/2^-$  isomer as indicated in the figure legend. This choice of gates excluded interference from the much more intense 424.9 keV transition and gave rather transparent summed spectrum of Fig. 4, which displays the new 395.5 keV transition depopulating the isomer, whereas the most intense other decay branches are practically absent.

Spectra displayed in Fig. 5 are focused on the identification of the new  $23/2^-$ , 3510.0 keV level, which is predominantly depopulated by the 937.9 keV transition to the  $19/2^-$ , 2572.1 keV level. Crucial energy regions of the coincidence spectrum obtained with double gate placed on the 378.4 and 937.9 keV transitions are displayed in Fig. 5(a) and can be compared with the corresponding parts of the projection spectrum displayed below in Fig. 5(b). In the low-energy part of Fig. 5(a) one observes the 181.8 keV transition populating the  $23/2^-$  3510.0 keV level from the well-established  $25/2^-$ , 3691.7 keV level. Here, the use of the  $\gamma\gamma\gamma$  coincidence cube with narrow selection of the prompt time window helped to obtain this clear evidence, in spite of a potentially disturbing presence of a much stronger 937.2 keV transition in the upper part of the level scheme and the dominance of the 182.9 keV transition (see the projection spectrum) which is nearly factor 60 more intense than the 181.8 keV transition clearly shifted down in energy. On the other hand, the strongly increased intensity ratio of the 1575.1 keV and 1491.0 keV transition observed in the Fig. 5(a) spectrum compared to the projection spectrum displayed below, confirms the placement of the 937.9 keV transition as populating the  $19/2^-$ , 2572.1 keV level. Later it turned out that the  $23/2^-$  3510.0 keV level is also weakly populated in the  $27/2^-$  isomer decay. In the low-energy spectrum obtained with double gate placed on the 937.9 and 1491.0 keV transitions and displayed in the Fig. 5(c), this 71.8 keV  $E2$  isomeric decay branch can be observed

along with the known 83.9 keV  $E1$  transition. Although the low statistics did not allow us to determine directly the  $\gamma$  intensity of this transition, it could be calculated using the total transition intensity extracted from the observed population of the 3510.0 keV level in the  $27/2^-$  isomer decay. In addition to the 937.9 keV main  $E2$  branch, three other much weaker 323.8, 471.9, and 749.7 keV  $E1$  transitions depopulating the 3510.0 keV  $23/2^-$  level could be firmly placed. Spectrum displayed in Fig. 5(d) and obtained with double gate placed on the 378.4 and 323.8 keV transitions shows the evidence for the placement of the weakest one of those  $E1$  branches.

It was concluded that in both of the earlier studies [18,19] the strong low-energy 80.4 keV transition was wrongly placed and this led to severe inconsistencies of the presented level schemes. In the present work this transition was firmly placed as feeding directly the  $31/2^+$ , 4948.6 keV level and the evidence is shown in spectra displayed in Fig. 6. In Fig. 6(b) spectrum obtained with double gate placed on the 80.4 and 330.8 keV transitions, the 1036.1 keV line represents the depopulation intensity of this positive parity sequence of yrast levels. A number of other lines seen in this spectrum and arising from parallel decay branches populating the 5029.0 keV,  $33/2^+$  level from above, establish the present placement of the 80.4 keV transition as the main decay branch from this level. The existence of the 5029.0 keV level is further confirmed by the identification of two other much weaker depopulating transitions (see Table III). Moreover, the double gate placed on the 591.1 and 1286.7 keV transitions selects one of the intense branches feeding the 5029.0 keV level from above and gave the spectrum displayed in Fig. 6(a), which shows the main 80.4, 330.8, and 1036.1 keV sequence of positive parity yrast states decay.

Finally, the coincidence spectra displayed in Figs. 7 and 8 are selected to demonstrate the resolving power, which was achieved in the analysis of the most complex high-energy part



FIG. 1. Upper part of the  $^{177}\text{Gd}$  isomeric decay. See caption of Fig. 2, which displays the lower part of the decay.



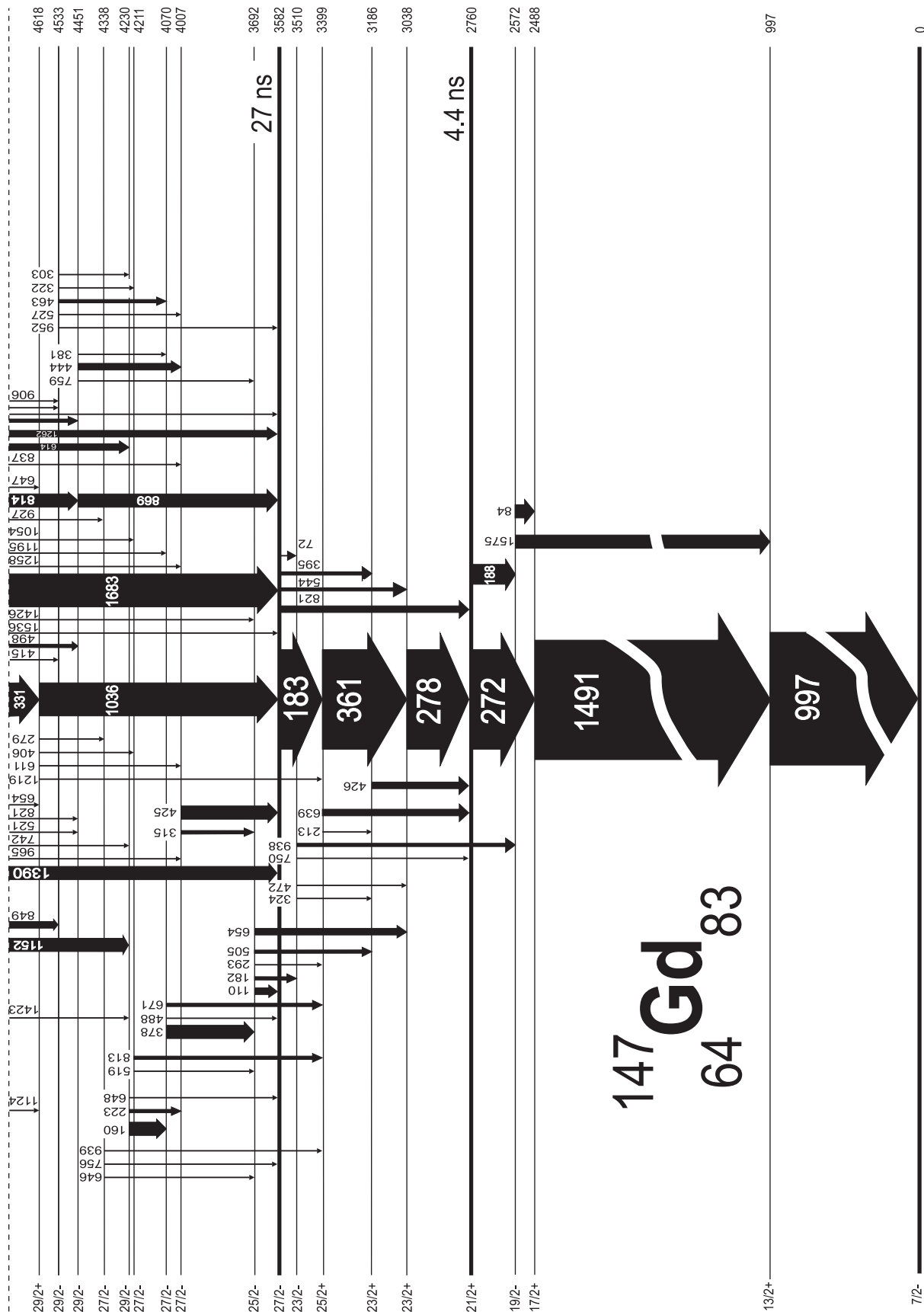


FIG. 2. Presently established decay scheme of the  $49/2^+$ , 510 ns isomer in  $^{147}\text{Gd}$ . The top part of the scheme is shown in Fig. 1. Arrow thickness indicates gamma intensity only for strongest transitions. For details see Table III and text.

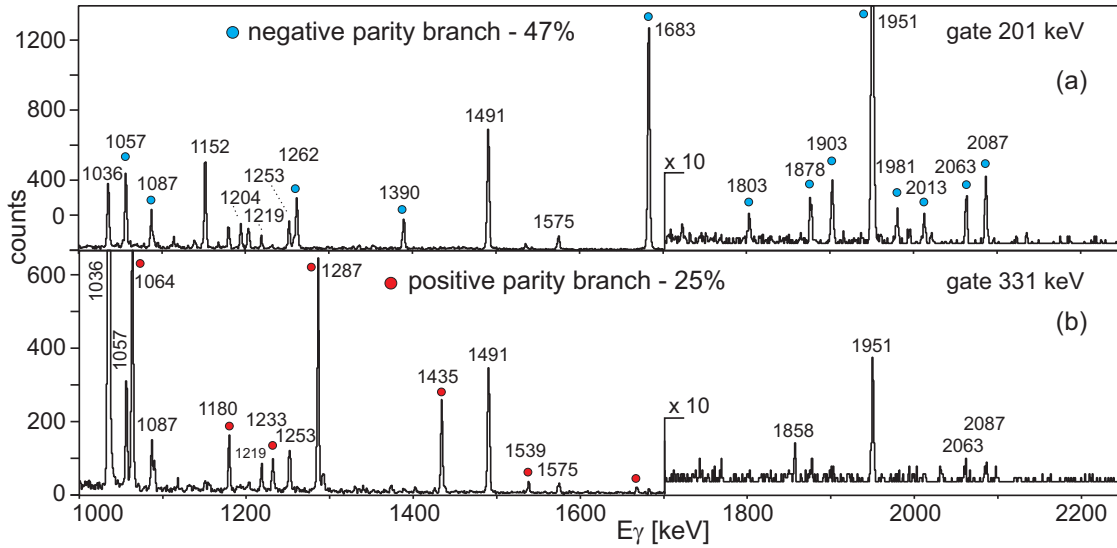


FIG. 3. Spectra of high-energy  $\gamma$  transitions populating the (a) negative and (b) positive parity main yrast levels. In the  $\gamma\gamma$  matrix preselected by requiring delayed coincidences with transitions below the  $27/2^-$  isomer, gates were placed on the 201 and 331 keV transitions representing 47% and 25% decay intensity, which populates (a) negative and (b) positive parity states, respectively (see text).

of the decay scheme. Gates placed on the two high-energy transitions 2086.8 and 2063.0 keV in the  $\gamma\gamma$  coincidence matrix of transitions preceding in time the  $27/2^-$  isomer decay, gave spectra, which are displayed in Fig. 7(a) and 7(b) and show, respectively, the 204.4 and 228.1 keV coincident transitions of less than 1% intensity and hardly visible in the matrix projection spectrum. In Fig. 8 the gates were placed in the same matrix on the 1090.7 keV [Fig. 8(a)] and 1194.9 keV [Fig. 8(b)] transitions depopulating the 8125.9 and 7666.2 keV levels, respectively. The 207.4 keV transition seen in spectrum [Fig. 8(a)] is clearly different from the 207.7 keV transition observed in the lower spectrum [Fig. 8(b)] and both components of the resolved doublet with energy difference of 0.3 keV are firmly placed in the level scheme. These placements are supported by the indicated absence of the

339.1 keV transition in spectrum (a), which depopulates the same 8333.3 keV level as 207.4 keV transition and by a presence in spectrum (b) of the 327.9 keV transition feeding the same 7666.2 keV level as the 207.7 keV transition. The presented examples show the standard way in which the level scheme was constructed to get the most complete picture of the  $^{147}\text{Gd}$   $49/2^+$  isomeric decay summarized fully in Table III. The earlier anticipated complexity of this decay [18] was confirmed and it is emphasized by a presence of several levels depopulated by more than 10 decay branches, up to 26 transitions depopulating the 7873.9 keV level. As mentioned before, the spin-parity assignments were based on all the earlier available results [18,19], and on the presently extracted total conversion coefficients of Table II, as well as on the observed pattern of  $\gamma$  transitions connecting the level with the already assigned ones. In Table III one may see that apart from few exceptions, the spin parity of all of the observed levels could be uniquely assigned.

## IV. DISCUSSION

### A. Shell-model states interpretation

The  $27/2^-$ , 3581.7 keV isomer in  $^{147}\text{Gd}$  and levels populated in its decay have been extensively discussed in Ref. [3] by considering the coupling of the  $f_{7/2}$  neutron with the  $\pi(h_{11/2})^2$  state and proton particle-hole excitations observed as the yrast level sequence in  $^{146}\text{Gd}$ . Within this picture the unobserved earlier second  $23/2^+$  level at 3186.1 keV, reported already in Ref. [18] but firmly assigned in the present work, completes the analogy reflecting the presence of the two close-lying  $8^-$  levels in  $^{146}\text{Gd}$ . Whereas it has been concluded in Ref. [3] that both  $8^-$  levels, the lower one with predominant  $\pi h_{11/2}d_{5/2}^{-1}$  and the higher one of  $\pi h_{11/2}g_{7/2}^{-1}$  structures, are practically not mixed, such mixing may occur for the two  $23/2^+$  levels when the  $f_{7/2}$  neutron is coupled to the  $8^-$  proton

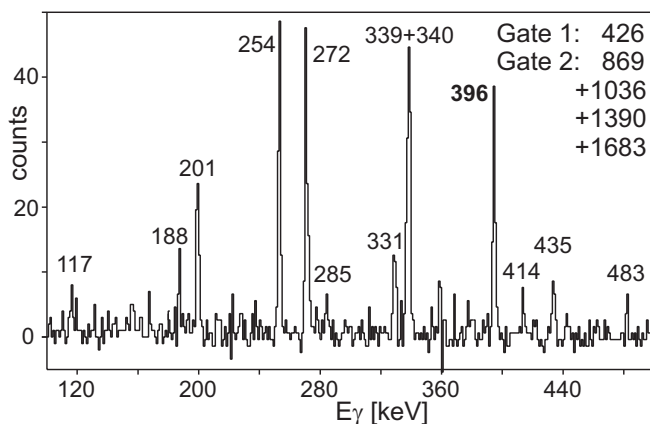


FIG. 4. Spectrum showing the presence of the 396 keV  $M2$  branch in the  $27/2^-$  isomer decay. In the  $\gamma\gamma\gamma$  cube the first gate was placed on the 426 keV transition and the second one on the four strongest transitions populating directly the  $27/2^-$  isomer (see text).

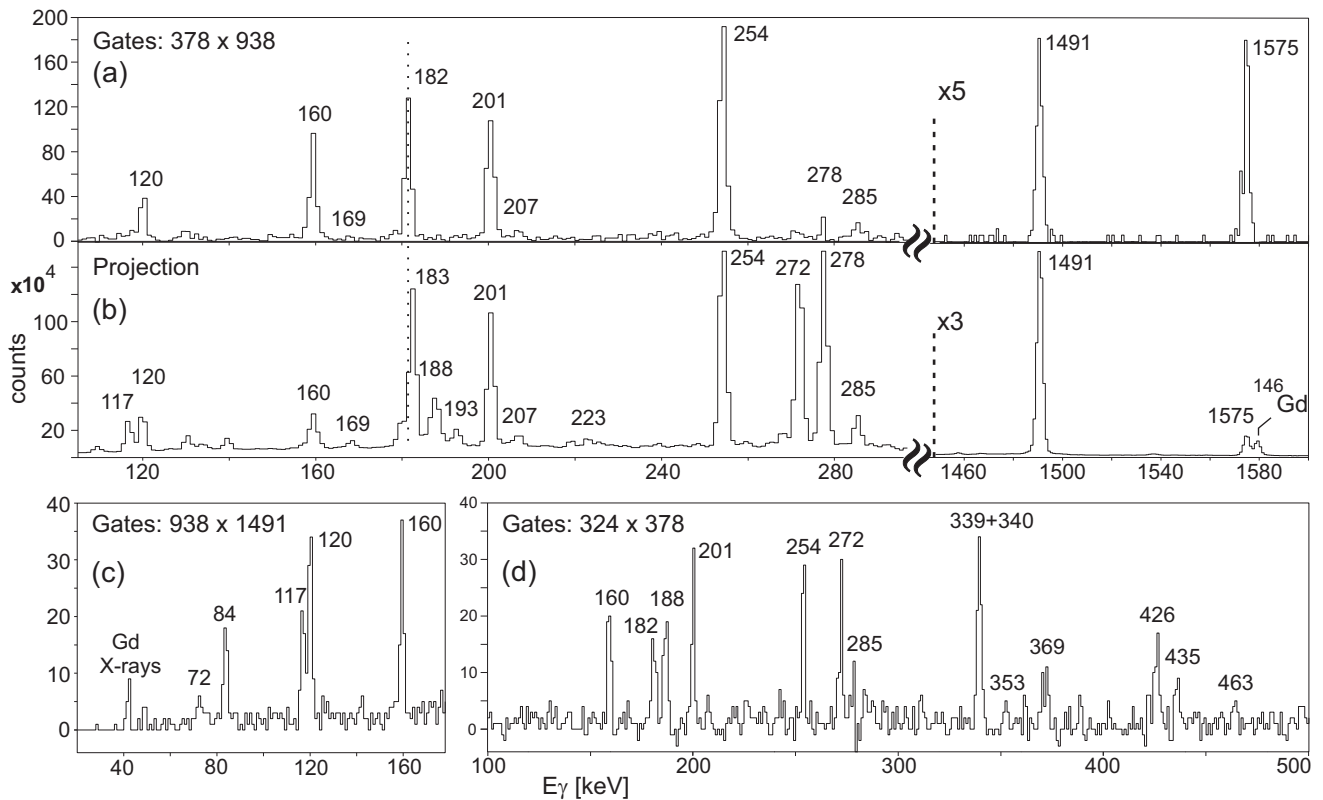


FIG. 5. Spectra documenting the existence of the 3510.0 keV  $23/2^-$  level. Important energy regions displayed in the (a) spectrum and obtained with double gate placed on the 378- and 938 transitions may be compared with the (b) projection spectrum displayed below to observe the main population of the state by the 182 keV transition passing by the  $27/2^-$  isomer. Low-energy part of the spectrum displayed in (c) shows the weak  $E2$  branch populating this level in the  $27/2^-$  isomer decay. Spectrum displayed in (d) proves the existence of the weakest 323 keV of the four transitions depopulating the 3510.0 keV level (see text).

excitations in  $^{147}\text{Gd}$ . The  $B(M2)$  rates of  $M2$  transitions populating both levels in the  $27/2^-$  isomer decay should then indicate the involvement of the  $g_{7/2}$  and  $d_{5/2}$  proton holes in their structure, taking into account expected rates of the allowed  $h_{11/2} \rightarrow g_{7/2}$  and forbidden  $h_{11/2} \rightarrow d_{5/2}$  transitions. In Ref. [3] only the 543.7 keV  $M2$  branch was observed and the extracted  $B(M2)$  value allowed us to estimate that the lower  $23/2^+$ , 3038.0 keV level contains 35% of the  $g_{7/2}$ -type configuration, whereas the main part of it was anticipated to be involved in the structure of the unobserved second  $23/2^+$  level. In the present work this second  $23/2^+$ , 3186.1 keV level was observed to be populated by the 395.5 keV  $M2$  transition in the  $27/2^-$  isomer decay (see Fig. 4). In Table IV list, which includes the reduced rate values extracted for all isomeric transitions depopulating the  $27/2^-$  and  $49/2^+$  isomers, the  $B(M2)$  value of the 395.5 keV  $M2$  is nearly factor two smaller than the one determined for the 543.7 keV  $M2$  branch. Thus, the earlier anticipation was probably not correct and the main amplitude of the  $g_{7/2}$ -type configuration has to be assigned rather to the lower  $23/2^+$  state structure.

The new  $23/2^-$ , 3510.0 keV level firmly located and assigned in this work is also populated in the  $27/2^-$  isomer decay by the weak 71.8 keV  $E2$  transition. The  $B(E2)$  value of this  $E2$  branch (see Table IV) is 3.5 times smaller than the  $B(E2)$  of the isomeric  $10^+ \rightarrow 8^+$  transition in  $^{148}\text{Dy}$  [4],

which indicates that the  $\pi h_{11/2}^2 \nu f_{7/2}$  configuration is probably not the main part of the  $23/2^-$  level structure. Moreover, the 181.8 keV  $M1$  transition populating this level from the  $25/2^-$ , 3691.7 keV of apparent  $\pi h_{11/2}^2 \nu f_{7/2}$  structure, is by factor 10

TABLE IV. Reduced transition rates for transitions depopulating the  $27/2^-$  and  $49/2^+$  isomers in  $^{147}\text{Gd}$ . Indicated level half-lives adopted from the previous investigations and the depopulation branching determined in the present work were used.

| $E_\gamma$<br>[keV]                              | $\sigma\lambda$ | $B(\sigma\lambda)$       |                |                          |
|--|-----------------|--------------------------|----------------|--------------------------|
|  |                 | Value                    | Units          | Value in W.u.            |
| Level 3581.7 keV $27/2^-$ $T_{1/2} = 26.8(7)$ ns |                 |                          |                |                          |
| 71.8   | $E2$            | 12.3(28)                 | $e^2 fm^4$     | 0.26(6)                  |
| 182.9  | $E1$            | $1.97(6) \times 10^{-6}$ | $e^2 fm^2$     | $1.10(4) \times 10^{-6}$ |
| 395.5  | $M2$            | 2.77(20)                 | $\mu_N^2 fm^2$ | 0.060(4)                 |
| 543.7  | $M2$            | 5.28(28)                 | $\mu_N^2 fm^2$ | 0.115(6)                 |
| 821.3  | $E3$            | 8247(220)                | $e^2 fm^6$     | 6.43(17)                 |
| Level 8587.7 keV $49/2^+$ $T_{1/2} = 510(20)$ ns |                 |                          |                |                          |
| 254.4  | $E2$            | 0.865(34)                | $e^2 fm^4$     | 0.0188(7)                |
| 434.5  | $E2$            | 0.00416(34)              | $e^2 fm^4$     | $9.0(7) \times 10^{-5}$  |
| 593.7  | $E3$            | 2524(142)                | $e^2 fm^6$     | 1.97(11)                 |
| 623.8  | $E3$            | 86(21)                   | $e^2 fm^6$     | 0.067(16)                |

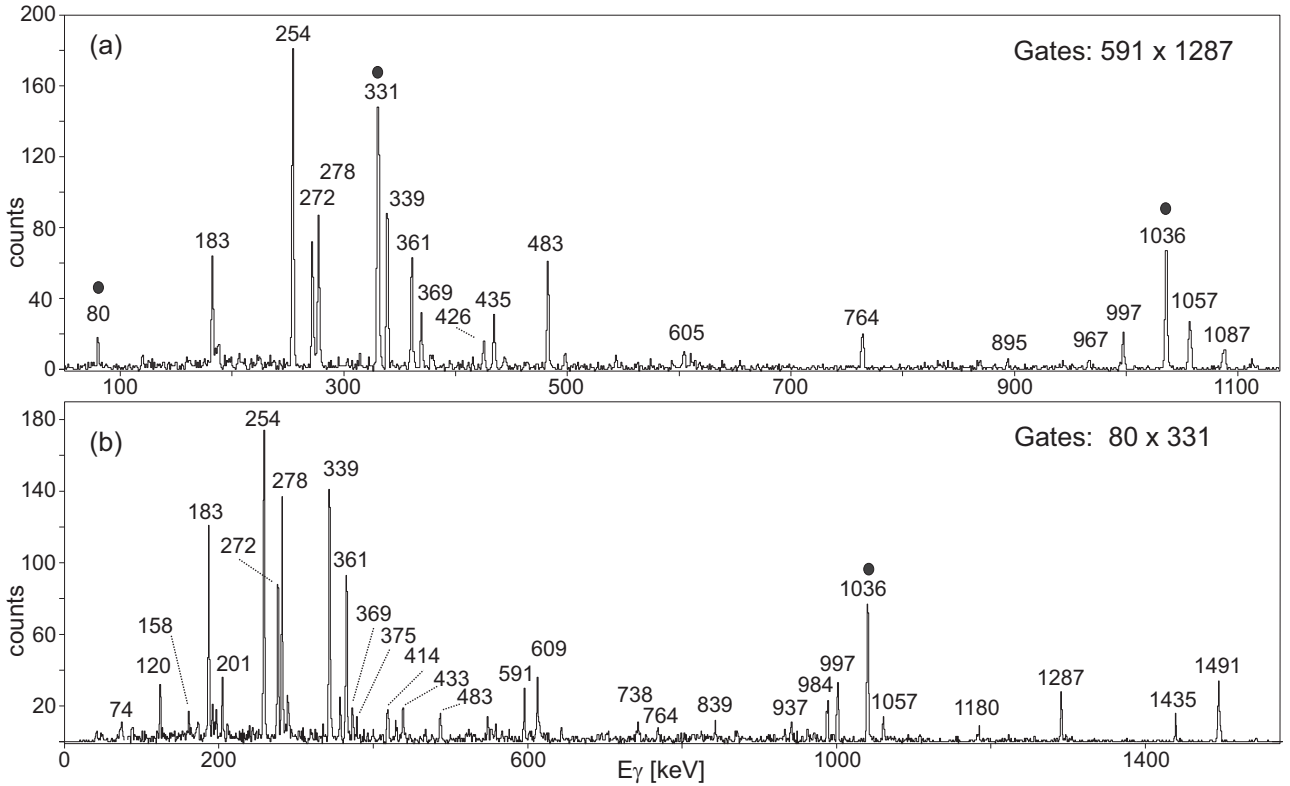


FIG. 6. Coincidence spectra obtained with double gates placed on  $\gamma$  transitions indicated in (a) and (b) legends verifying the present revised placement of the 80 keV transition in the positive parity yrast sequence (see text).

slower than the competing 110.0 keV  $M1$  transition to the  $27/2^-$  isomer. Much more likely this  $23/2^-$  level should then be considered as arising from the coupling of the  $i_{13/2}$  neutron with the  $(h_{11/2}d_{5/2}^{-1})5^-$  proton excitation of  $^{146}\text{Gd}$ . In analogy to the 2572.1 keV  $19/2^-$  level discussed in Ref. [3] as the  $\nu i_{13/2} \otimes 3^-$  excitation, the  $23/2^-$  level most likely has the  $\nu i_{13/2} \otimes 5^-$  structure. With the most intense 937.9 keV  $E2$  branch depopulating this state to the  $19/2^-$  level the sequence of 938–1575 keV transitions above the  $13/2^+$  997.1 keV level resembles well the  $5^- \rightarrow 3^- \rightarrow 0^+$ , 1079–1579 keV sequence known in  $^{146}\text{Gd}$ .

Above the  $27/2^-$  isomer many negative parity levels are strongly populated and only one sequence of positive parity states competes in gaining yrast population. These are positive parity levels arising by coupling the octupole core excitation with the  $27/2^-$  isomeric level structure, which involves the  $(h_{11/2})^2 10^+$  pair of protons and blocks by Pauli interference the main  $(h_{11/2}d_{5/2}^{-1})3^-$  component in higher spin states. This coupling was discussed in detail in Ref. [4] and the sequence of 3647, 3887, and 4086 keV levels, assigned in  $^{149}\text{Dy}$  as  $29/2^+$ ,  $31/2^+$ , and  $33/2^+$  states, respectively [6], allows us to expect a similar sequence of the three levels above the  $27/2^-$  isomer in  $^{147}\text{Gd}$ . The present correct placement of the 80.4 keV transition depopulating the 5029.0 keV,  $33/2^+$  level and the subsequent decay via the 4948.6 keV  $31/2^+$  and 4617.8 keV  $29/2^+$  levels down to the 3581.7 keV  $27/2^-$  isomer establishes clearly a similar structure of positive parity levels in  $^{147}\text{Gd}$ . It may be noted that in both cases the  $33/2^+$  levels are observed above the  $27/2^-$  isomers at similar energy

distances of 1423 and 1447 keV in  $^{149}\text{Dy}$  and  $^{147}\text{Gd}$ , respectively.

For negative parity levels above the  $27/2^-$  isomer the most effective way to gain spin requires breaking of the pair of proton holes that are present in the isomer structure. These holes located on the  $d_{5/2}$  and  $g_{7/2}$  orbitals provide up to six units of spin at energy cost up to 2324 keV energy of the  $6^+$  level in  $^{144}\text{Sm}$  [23]. Such structure can be clearly attributed to the sequence of strongly populated yrast levels 6471.3 ( $39/2^-$ ), 5922.9 ( $37/2^-$ ), 5582.8 ( $35/2^-$ ), 5382.1 ( $33/2^-$ ), 5264.9 keV, ( $31/2^-$ ), which are connected by intense  $M1$  transitions and finally depopulate to the  $27/2^-$  isomer by the strong 1683.3 keV  $E2$  transition resembling closely the 1660 keV  $E2$  decay of the  $2^+$  level in  $^{144}\text{Sm}$  [23].

## B. Origin of the observed decay complexity

Whereas for a large number of other  $^{147}\text{Gd}$  levels similar consideration of the level structure would be too speculative, one may try to understand the origin of the observed shower of  $\gamma$  rays and established phenomenon of an extraordinary complexity of the  $49/2^+$  isomer decay. In the level scheme region where the most complex branching occurs, three levels with largest number of depopulating transitions could be selected to compare the decay rates: 7994.2 keV,  $43/2^-$ , 7873.9 keV,  $41/2^-$ , and 7825.6 keV,  $41/2^-$ , depopulated by 20, 26, and 15 competing transitions, respectively. Although the level lifetimes are not known, one may compare the relative  $B(M1)$  and  $B(E1)$  reduced rates for all  $M1$  and  $E1$  transitions assigned

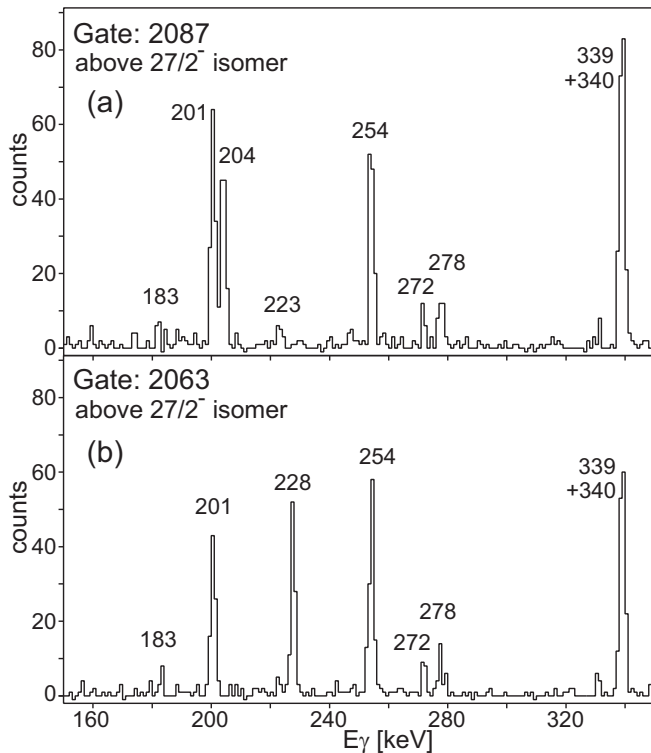


FIG. 7. Low-energy parts of coincidence spectra obtained with gates placed on (a) 2087 and (b) 2063 keV transitions in the  $\gamma\gamma$  matrix preselected by requiring delayed coincidences with transitions below the  $27/2^-$  isomer. The spectra demonstrate the resolving power as the observed 204 keV (a) and 228 keV (b) transitions have intensities less than 1%.

among branches depopulating each of these three levels. The measured  $\gamma$ -transition intensities divided by the  $E_\gamma^3$  energy factors provide the relative values of the reduced rates in arbitrary units. In Table V these calculated values are listed separately for the  $M1$  and  $E1$  transitions depopulating the three selected levels mentioned above. In all cases one may observe few low-energy  $M1$  transitions with  $B(M1)$  rates, which are orders of magnitude larger than the higher-energy  $M1$  transitions. This is particularly clearly seen in the case of the 7873.9 keV  $41/2^-$  level with 16 assigned  $M1$  branches, where the two lowest-energy transitions exhibit  $B(M1)$  rates up to three orders of magnitude larger than the long tail of values determined for higher-energy  $M1$  transitions. In the same time the competing  $E1$  transitions show rather flat distribution of the relative  $B(E1)$  rates listed in Table V. This analysis allows us to understand the general structural features, which are at the origin of the observed extraordinary complexity of the investigated  $^{147}\text{Gd}$   $49/2^+$  isomeric decay. The decay of the isomer with well-defined  $[\pi d_{5/2}^{-2} h_{11/2}^2] 110 [v h_{11/2}^{-1} i_{13/2} f_{7/2}] 29/2$  configuration and large oblate deformation is initiated by the two  $E2$  and two  $E3$  isomeric transitions (reduced transition rates are indicated in Table IV), which depopulate the isomer to the two  $45/2^+$  and two  $43/2^-$  available levels. Already at these two  $43/2^-$  levels the complex branching starts and is subsequently multiplied by even more complex depopulation of several close-lying lower-energy levels. Apparently many

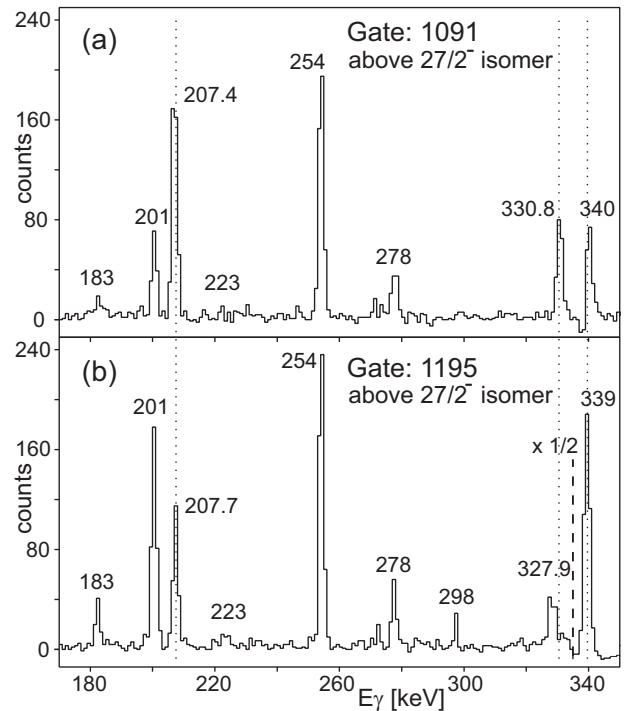


FIG. 8. Examples of coincidence spectra selected as in Fig. 7 to demonstrate the resolving power of the present data. The gates were placed on the (a) 1091 keV and (b) 1195 keV transitions using the same  $\gamma\gamma$  matrix involving transitions above the  $27/2^-$  isomer. The 207.4 and 207.7 keV observed in the spectrum (a) and (b), respectively, shows the resolved doublet of transitions separated by 0.3 keV (see text for more details).

of these levels are of very similar structure, since they are connected by fast  $M1$  transitions distinguished by the large  $B(M1)$  reduced transition rates discussed above. On the other hand, the grouping of similar structure levels in the narrow excitation energy range defines the very low energy of the connecting fast  $M1$  transitions and this enables many much slower, but higher-energy  $M1$  and  $E1$  transitions to compete in the observed depopulation and spread the decay to many lower-energy levels with more different structures. One may conclude that the main origin of the observed complexity in the  $^{147}\text{Gd}$  isomer decay is the presence of a group of levels in the narrow 7.8–8.0 MeV excitation energy range, which have similar structures and are connected by fast  $M1$  transitions. In this group of levels the extraordinary branching is initiated and then it is multiplied in the subsequent depopulation dictated by usual rules of  $\gamma$  decays.

## V. SOME STATISTICAL FEATURES OF THE $49/2^+$ ISOMER DECAY

Probably only in the  $(n, \gamma)$  neutron capture experiments one observes a similarly complex depopulation of single levels in nuclei that are produced in nuclear reaction. For example, in the  $^{209}\text{Bi}(n, \gamma)$  thermal neutron capture 64 primary transitions were identified as depopulating the unresolved  $4^-$  and  $5^-$  states in the final  $^{210}\text{Bi}$  nucleus [24]. Whereas in these reactions the low-spin states are selectively populated

TABLE V. For three levels exhibiting the largest numbers of depopulating transitions the relative reduced transition rates of  $M1$  and  $E1$  transitions are compared. For the listed  $M1$  and  $E1$  transitions depopulating each level, the  $I_\gamma/E^3$  values were calculated using the  $I_\gamma$  intensities of Table I and transition energy  $E$  in MeV. These values listed in columns 2 and 4 represent the reduced transition rates in arbitrary units different for each state.

| $M1$                      |                | $E1$                |                |
|---------------------------|----------------|---------------------|----------------|
| $E_\gamma$<br>[keV]       | $I_\gamma/E^3$ | $E_\gamma$<br>[keV] | $I_\gamma/E^3$ |
| Level 7994.1 keV $43/2^-$ |                |                     |                |
| 30.4                      | 231570         | 302.4               | 22             |
| 77.2                      | 870            | 374.5               | 57             |
| 90.8                      | 1200           | 463.3               | 159            |
| 120.2                     | 128400         | 598.2               | 89             |
| 168.6                     | 5570           | 605.0               | 130            |
| 192.9                     | 4500           | 641.8               | 10             |
| 327.9                     | 179            | 958.9               | 45             |
| 781.7                     | 33             | 1087.4              | 28             |
| Level 7873.9 keV $43/2^-$ |                |                     |                |
| 48.3                      | 56800          | 838.7               | 82             |
| 72.7                      | 37480          | 937.2               | 49             |
| 73.7                      | 4500           | 967.1               | 29             |
| 105.5                     | 341            | 979.2               | 21             |
| 155.5                     | 399            | 1035.4              | 6              |
| 168.2                     | 84             | 1252.7              | 19             |
| 204.4                     | 1065           |                     |                |
| 207.7                     | 926            |                     |                |
| 228.1                     | 615            |                     |                |
| 278                       | 79             |                     |                |
| 566.3                     | 23             |                     |                |
| 598.7                     | 12             |                     |                |
| 691.1                     | 13             |                     |                |
| 747.2                     | 41             |                     |                |
| 855.8                     | 3              |                     |                |
| 1215.7                    | 1              |                     |                |
| Level 7825.6 keV $41/2^-$ |                |                     |                |
| 119.8                     | 465            | 790.3               | 44             |
| 229.7                     | 404            | 888.7               | 4.0            |
| 517.8                     | 23             | 919                 | 2.4            |
| 550.3                     | 14             | 1204.5              | 4.3            |
| 699                       | 3.5            |                     |                |
| 1102.4                    | 0.5            |                     |                |
| 1167.9                    | 1.8            |                     |                |
| 1354                      | 0.6            |                     |                |

in the excitation energy range, which is characterized by high density of levels, the subsequent depopulation initiated by primary transitions is less complex and proceeds essentially through all levels with spin-parity values available for the  $\gamma$  decay. In the case of high-spin isomers the decay complexity established in the present study of the  $^{147}\text{Gd}$  isomer was not observed before and with the number of 400 observed  $\gamma$  transitions and 91 identified levels simple statistical considerations may be appropriate for summarizing general features of the investigated decay.

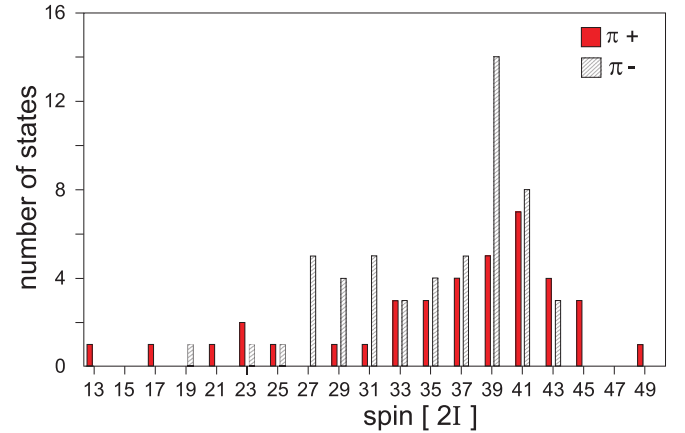


FIG. 9. Number of observed and assigned levels for each spin value and parity.

The branching of transitions depopulating each of the levels listed in Table III allows us to follow the selected paths of the  $^{147}\text{Gd}$  decay from the  $49/2^+$  isomeric state down to the  $7/2^-$  ground state. Following the most probable decay way, which involves the sequence of the 14 most intense transitions, one calculates that the probability of this most frequent decay way is only  $1.17 \times 10^{-2}$ /decay. In a similar way one finds the shortest way of the decay, which includes only 10 transitions (three of them  $E3$ ) and happens with probability  $1.5 \times 10^{-6}$ , as well as the longest one involving 22 transitions and probability calculated as  $5.3 \times 10^{-7}$ /decay. Whereas the total number of the decay ways is extremely large, one may follow few of those involving weakest transition branches, which are calculated to happen with the lowest probability in the  $10^{-17}$ /decay range. Although the possibility to detect such cases in experiment is obviously excluded, the branching established at each level allows us to calculate safely their extremely low probabilities. Consideration of the statistical distribution of probabilities for different established decay ways, which range between  $10^{-2}$  and  $10^{-17}$ /decay would require more advanced analysis. Here, the expected complexity may be emphasized by considering the contribution from the last fraction of the whole decay, which takes place below the  $27/2^-$  isomer. The relatively simple decay scheme in this fraction involves 26 decay ways that proceed with probability ranging from 0.61 to  $10^{-5}$ /decay. Consequently, the extremely large number of the observed decay ways between the  $49/2^+$  and  $27/2^-$  isomers will have to be multiplied by these 26 possible final decay ways, each of them taking place with the well-determined probability. An interesting result of the present investigation is the identification of the 89 fully assigned levels in  $^{147}\text{Gd}$  between the isomer and ground state, compared to the 38 earlier established ones, some of which had to be presently revised. The distribution displayed in Fig. 9 shows numbers of observed levels for both parities at each spin value from  $I = 13/2$ – $49/2$ . Although for nearly all spin values one observes yrast and several higher-lying levels, the largest number of 19 and 15 observed levels with  $39/2$  and  $41/2$  spin values, respectively, reflects the main branching of the depopulation, which occurs in the narrow

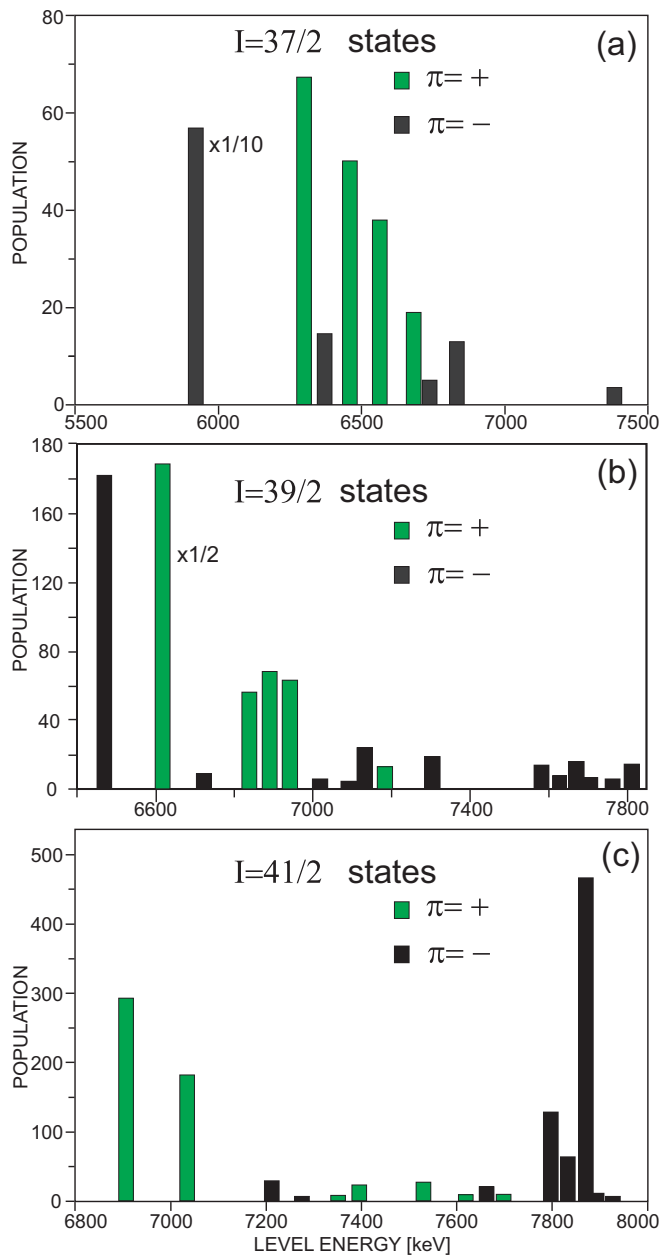


FIG. 10. Population intensity versus excitation energy observed for all levels assigned with spin values (a) 37/2, (b) 39/2, (c) 41/2 and both parities.

energy and spin ranges as discussed earlier in Sec. IV. More detailed pictures are presented in Figs. 10(a), 10(b) 10(c) showing the observed population intensity for all levels with spin values 37/2, 39/2, and 41/2 and each parity. One may see that in all cases levels are populated within a broad range of excitation energies above the yrast states and for the  $I^\pi = 41/2^-$  the predominantly populated levels are located 0.7 MeV higher than the yrast state. This reemphasizes the earlier concluded explanation of the origin of the observed decay complexity.

The present work is focused on experimental results and the discussion of the level structure in few cases did not

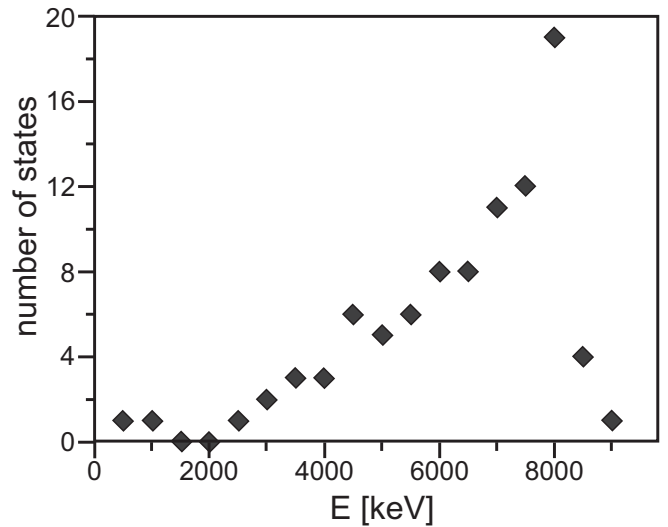


FIG. 11. Number of levels observed within 0.5 MeV excitation energy bins.

involve any theoretical calculations. Whereas the expected accuracy of the presently available shell-model calculations can hardly provide detailed understanding of many of the observed levels, the emerging complexity of the  $^{147}\text{Gd } 49/2^+$  isomeric decay might be used to inquire statistical aspects that may touch more fundamental problem. It is well known that with the increasing density of states at higher excitation energies, up to the unresolved continuum, the quantum physics description of many observed phenomena for practical reasons has to be replaced by classical physics tools, e.g., thermodynamics describes neutron evaporation from the strongly excited compound nucleus. The situation is clearly different in the present case where the decay of one single isomeric state with well-defined structure initiates a very complex  $\gamma$  decay down to the  $^{147}\text{Gd}$  ground state. Although levels populated in this decay are all well resolved and each of them is a discrete level with the structure that can be calculated using the quantum physics tools, the large numbers of observed 91 levels and 400  $\gamma$  transitions presents an opportunity to look for statistical features, which possibly might smear out the quantum physics picture. In Fig. 11 the number of observed levels as a function of excitation energy is displayed in 0.5 MeV bins. Whereas the picture is similar to the increasing density of selected spin states with excitation energy, it represents the density of levels in a broad spin range populated in the isomeric state decay. The displayed distribution does not show any irregularity that could be expected within the quantum physics picture. Another arbitrarily selected example is presented in Fig. 12(a), where the number of transitions of any intensity (see Table I), observed within 0.1 MeV energy bins is displayed for the whole measured transition energy range. Also this distribution is continuous and does not show irregularities, which could indicate quantum physics effects, except for a weak maximum observed around 2 MeV excitation energy. In Fig. 12(b) the summed total intensity of all transitions within each energy bin is displayed and this distribution seems to show some irregularities when the

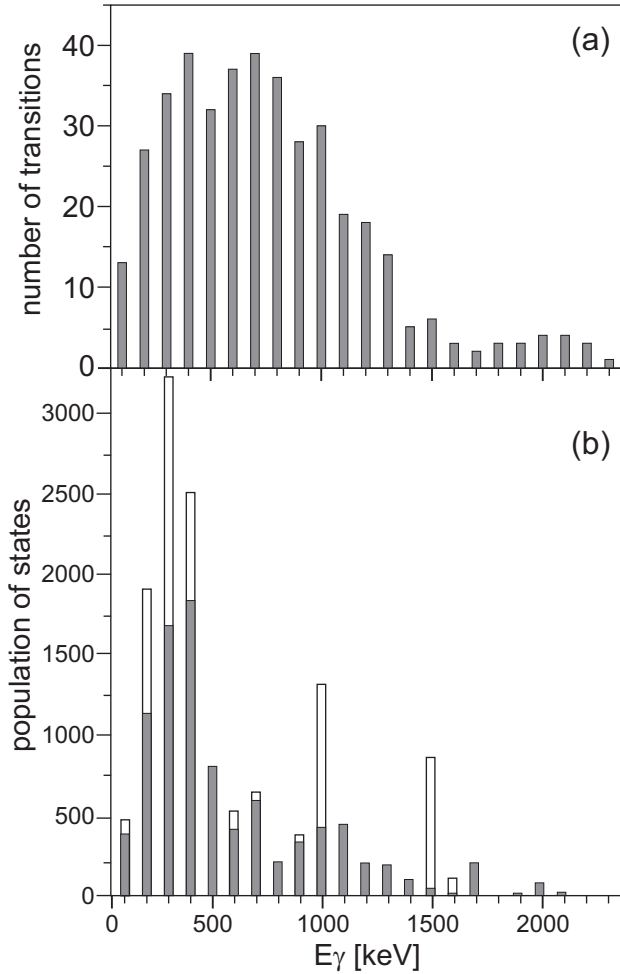


FIG. 12. Number of transitions identified in the decay scheme within (a) 0.1 MeV bins and (b) the summed total intensity of these transitions. Filled and empty bars in (b) represent intensities with excluded and included transitions below  $27/2^-$  isomer, respectively.

intensities correlated with level structure properties are included. Here, the transitions below the  $27/2^-$  isomer were excluded, since their predominant intensities strongly affect the picture with irregularities. Inclusion of these transitions gives points marked by empty bars in Fig. 12(b) allowing us to see the contribution characteristic for discrete states of well-defined structure populated in the  $27/2^-$  isomer decay, which is absent in the much more statistical decay above this isomer.

## VI. CONCLUSIONS

The  $49/2^+$ ,  $T_{1/2} = 510$  ns isomeric decay in  $^{147}\text{Gd}$  was reinvestigated in a catcher experiment, using the  $^{76}\text{Ge}(^{76}\text{Ge}, 5n)$  reaction and the GASP detector array at the Legnaro NL. The extraordinary complexity of the decay anticipated from earlier investigation was fully confirmed by establishing 89 levels populated in the decay between the  $49/2^+$  isomer and the  $7/2^-$  ground state. The coincidence data allowed us to identify 400  $\gamma$  transitions, which were firmly placed in the decay scheme including those with in-

tensities ranging below the  $10^{-3}$ /decay level. The electron conversion coefficients and  $\gamma$  angular distribution results available from previous investigations [18,19] as well as the present determination of the total electron conversion coefficients from the observed intensity balance provided spin-parity assignments for all of the observed levels. The level structure was qualitatively discussed in few selected cases where the present results clarified the previously incomplete experimental information. Those included consideration of the  $27/2^-$  isomer decay in which two new  $M2$  and  $E2$  decay branches were established, the identification of a new  $23/2^-$  level below this isomer, the corrected identification of the yrast sequence of positive parity states involving octupole core excitation, as well as general consideration of the yrast negative parity levels up to  $I = 39/2$  spin value. The observed isomeric decay complexity is essentially initiated in the critical excitation energy range from 7.8–8.0 MeV and may be attributed to the presence of a narrowly spaced group of levels, which have similar structure and are connected by fast low-energy  $M1$   $\gamma$  transitions spreading the decay intensity. This was concluded from the comparison of relative transition rates for  $M1$  and  $E1$  branches observed in the decay of three levels in this energy region exhibiting the largest numbers of depopulating branches. Taking into account an extraordinary complexity of the established decay and rather unusual situation in which this shower of  $\gamma$  rays starts from a single high-spin state of well-defined structure, few statistical features were presented to summarize the obtained results. Considering different decay ways from the  $49/2^+$  isomer to the  $7/2^-$  ground state one finds the multiplicity of  $\gamma$  rays varying from 10–22 and the probability to follow a specific decay way, which can be selected from the extremely large number of possibilities, ranges from 1.2%/decay for the way involving the most intense transitions, down to the  $10^{-17}$ /decay probability when the decay follows by weakest branches. The distribution of number of levels populated in the decay shows surprisingly regular increase as a function of spin and excitation energy reaching maximum values around  $I = 41/2$  and 8 MeV, respectively. On the other hand, the displayed population intensity of the  $37/2$ ,  $39/2$ , and  $41/2$ , negative and positive parity levels distributed within a broad excitation energy ranges indicated rather scattered population without strong preference of yrast levels. The statistical distribution of a number of transitions identified within 0.1 MeV energy bins did not show any irregularities expected for the observable involving discrete levels that may be described within quantum physics. However, the decay intensity carried by these groups of transitions exhibits some irregularities apparently reflecting the structure of involved levels. More advanced statistical considerations were suggested to exploit the presented results in a search for a possible transition from the quantum to classical physics picture when large numbers of observables are available. Finally, the presently revealed isomeric decay complexity may explain difficulties encountered in efforts to locate the observed highest spin rotational bands in  $^{147}\text{Gd}$  [11,12]. The  $\gamma$  decay connecting these superdeformed states with the well-known normal deformation states may be fragmented in a similar way, and therefore very difficult to be detected.



## ACKNOWLEDGMENTS

The authors thank the Tandem and ALPI Linac operating staff of the Legnaro NL for the efficient running of the accelerator during the experiment performed for

the present study. This work was supported by the Polish National Science Centre under Contract No. UMO-2015/14/m/ST2/00738 (COPIN-INFN Collaboration) and in the early phase by the Grant under Contract No. 0086/B/H03/2011/40.

- 
- [1] P. Kleinheinz, S. Lunardi, M. Ogawa, and M. R. Maier, *Z. Phys. A* **284**, 351 (1978); P. Kleinheinz, M. Ogawa, R. Broda, P. J. Daly, D. Haenni, H. Beuscher, and A. Kleinrahm, *ibid.* **286**, 27 (1978).
- [2] M. Ogawa, R. Broda, K. Zell, P. J. Daly, and P. Kleinheinz, *Phys. Rev. Lett.* **41**, 289 (1978).
- [3] P. Kleinheinz, R. Broda, P. J. Daly, S. Lunardi, M. Ogawa, and J. Blomqvist, *Z. Phys. A* **290**, 279 (1979).
- [4] P. J. Daly, P. Kleinheinz, R. Broda, S. Lunardi, H. Backe, and J. Blomqvist, *Z. Phys. A* **298**, 173 (1980).
- [5] R. Broda, M. Behar, P. Kleinheinz, P. J. Daly, and J. Blomqvist, *Z. Phys. A* **293**, 135 (1978).
- [6] M. Gupta, Pragma Das, S. B. Patel, R. K. Bhowmik, T. Werner, and Y. A. Akovali, *Phys. Rev. C* **54**, 1610 (1996).
- [7] R. Broda, P. J. Daly, Z. W. Grabowski, H. Helppi, M. Kortelahti, J. McNeill, R. V. F. Janssens, R. D. Lawson, D. C. Radford, and J. Blomqvist, *Z. Phys. A: At. Nucl.* **321**, 287 (1985).
- [8] R. Broda, P. J. Daly, J. McNeill, R. V. F. Janssens, and D. C. Radford, *Z. Phys. A: At. Nucl.* **327**, 403 (1987).
- [9] B. Haas, D. Ward, R. A. Andrews, O. Häusser, A. J. Ferguson, J. P. Sharpey-Schafer, T. K. Alexander, W. Trautmann, D. Horn, P. Taras, P. Skensved, T. L. Khoo, R. K. Smither, I. Ahmad, C. N. Davids, W. Kutschera, S. Levenson, and C. L. Dors, *Nucl. Phys. A* **362**, 254 (1981).
- [10] J. Borggreen, G. Sletten, S. Björnholm, J. Pedersen, A. Del Zoppo, D. C. Radford, R. V. F. Janssens, P. Chowdhury, H. Emling, D. Frékers, and T. L. Khoo, *Nucl. Phys. A* **466**, 371 (1987).
- [11] B. Haas, V. P. Janzen, D. Ward, H. R. Andrews, D. C. Radford, D. Prevost, J. A. Kuehner, A. Omar, C. Waddington, T. E. Drake, A. Galindo-Uribarri, G. Zwartz, S. Flibotte, P. Taras, and I. Ragnarsson, *Nucl. Phys. A* **561**, 251 (1993).
- [12] Ch. Theisen, N. Khadiri, J. P. Vivien, I. Ragnarsson, C. W. Beausang, F. A. Beck *et al.*, *Phys. Rev. C* **54**, 2910 (1996).
- [13] J. Pedersen, B. B. Back, F. M. Bernthal, S. Björnholm, J. Borggreen, O. Christensen, F. Folkmann, B. Herskind, T. L. Khoo, M. Neiman, F. Pühlhofer, and G. Sletten, *Phys. Rev. Lett.* **39**, 990 (1977).
- [14] R. Broda, M. Ogawa, S. Lunardi, M. R. Maier, P. J. Daly, and P. Kleinheinz, *Z. Phys. A* **285**, 423 (1978).
- [15] O. Häusser, P. Taras, W. Trautmann, D. Ward, T. K. Alexander, H. R. Andrews, B. Haas, and D. Horn, *Phys. Rev. Lett.* **42**, 1451 (1979).
- [16] O. Häusser, H. E. Mahnke, T. K. Alexander, H. R. Andrews, J. F. Sharpey-Schafer, M. L. Swanson, D. Ward, P. Taras, and J. Keinonen, *Nucl. Phys. A* **379**, 287 (1982).
- [17] E. Dafni, J. Bendahan, C. Broude, G. Goldring, M. Hass, E. Naim, M. H. Rafailovich, C. Chasman, O. C. Kistner, and S. Vajda, *Nucl. Phys. A* **443**, 135 (1985).
- [18] R. Broda, P. Kleinheinz, S. Lunardi, J. Styczeń, and J. Blomqvist, *Z. Phys. A, Atoms and Nuclei* **305**, 281 (1982).
- [19] O. Bakander, C. Baktash, J. Borggreen, J. B. Jensen, K. Kownacki, J. Pedersen, G. Sletten, D. Ward, H. R. Andrews, O. Häusser, P. Skensved, and P. Taras, *Nucl. Phys. A* **389**, 93 (1982).
- [20] N. Nica, *Nucl. Data Sheets* **110**, 749 (2009).
- [21] C. Rossi Alvarez, in *Proceedings of the 5th International Spring Seminar on Nuclear Physics "New perspectives in nuclear structure"*, edited by A. Covello (World Scientific Press, Singapore, 1996), p. 417.
- [22] E. Browne and J. K. Tuli, *Nucl. Data Sheets* **110**, 507 (2009).
- [23] A. A. Sonzogni, *Nucl. Data Sheets* **93**, 599 (2001).
- [24] N. Cieplicka-Oryńczak, B. Fornal, S. Leoni, D. Bazzacco, A. Blanc, G. Bocchi, S. Bottoni, G. de France, M. Jentschel, U. Köster, P. Mutti, G. Simpson, T. Soldner, B. Szpak, C. Ur, and W. Urban, *Phys. Rev. C* **93**, 054302 (2016).